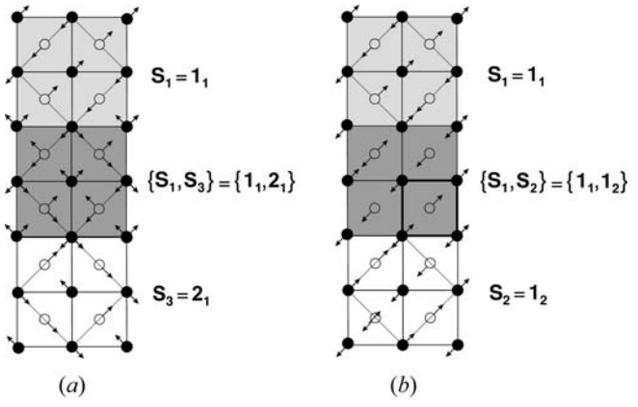

Fig. 3.4.3.10. Domain pairs in calomel. Single-domain states in the parent clamping approximation are those from Fig. 3.4.2.5. The first domain state of a domain pair is shown shaded in grey ('black'), the second domain state is colourless ('white'), and the domain pair of two interpenetrating domain states is shown shaded in dark grey. (*a*) Ferroelastic domain pair $(\mathsf{S}_1, \mathsf{S}_3)$ in the parent clamping approximation. This is a partially transposable domain pair. (*b*) Translational domain pair $(\mathsf{S}_1, \mathsf{S}_2)$. This is a completely transposable domain pair.

with symmetry descent $\bar{3}m \supset mmm$, where ferroelastic domain walls were detected only in thin samples.

3.4.3.7. *Domain pairs in the microscopic description*

In the *microscopic description*, two microscopic domain states S_i and S_k with space-group symmetries $\mathcal{F}_i$ and $\mathcal{F}_k$, respectively, can form an ordered domain pair $(\mathsf{S}_i, \mathsf{S}_k)$ and an unordered domain pair $\{\mathsf{S}_i, \mathsf{S}_k\}$ in a similar way to in the continuum description, but one additional aspect has to be considered. The definition of the symmetry group $\mathcal{F}_{ik}$ of an ordered domain pair $(\mathsf{S}_i, \mathsf{S}_k)$,

$$\mathcal{F}_{ik} = \mathcal{F}_i \cap \mathcal{F}_k, \tag{3.4.3.72}$$

is meaningful only if the group $\mathcal{F}_{ik}$ is a space group with a three-dimensional translational subgroup (three-dimensional *twin lattice* in the classical description of twinning, see Section 3.3.8)

$$\mathcal{T}_{ik} = \mathcal{T}_i \cap \mathcal{T}_k, \tag{3.4.3.73}$$

where $\mathcal{T}_i$ and $\mathcal{T}_k$ are translation subgroups of $\mathcal{F}_i$ and $\mathcal{F}_k$, respectively. This condition is fulfilled if both domain states S_i and S_k have the same spontaneous strains, *i.e.* in non-ferroelastic domain pairs, but in ferroelastic domain pairs one has to suppress spontaneous deformations by applying the parent clamping approximation [see Section 3.4.2.2, equation (3.4.2.49)].

Example 3.4.3.9. *Domain pairs in calomel.* Calomel undergoes a non-equitranslational phase transition from a tetragonal parent phase to an orthorhombic ferroelastic phase (see Example 3.4.2.7 in Section 3.4.2.5). Four basic microscopic single-domain states are displayed in Fig. 3.4.2.5. From these states, one can form 12 non-trivial ordered single-domain pairs that can be partitioned (by means of double coset decomposition) into two orbits of domain pairs.

Representative domain pairs of these orbits are depicted in Fig. 3.4.3.10, where the first microscopic domain state S_i participating in a domain pair is displayed in the upper cell (light grey) and the second domain state S_j, $j = 2, 3$, in the lower white cell. The overlapping structure in the middle (dark grey) is a geometrical representation of the domain pair $\{\mathsf{S}_1, \mathsf{S}_j\}$.

The domain pair $\{\mathsf{S}_1, \mathsf{S}_3\}$, depicted in Fig. 3.4.3.10(*a*), is a ferroelastic domain pair in the parent clamping approximation. Then two overlapping structures of the domain pair have a common three-dimensional lattice with a common unit cell (the dotted square), which is the same as the unit cells of domain states S_1 and S_3.

Domain pair $\{\mathsf{S}_1, \mathsf{S}_2\}$, shown in Fig. 3.4.3.10(*b*), is a translational (antiphase) domain pair in which domain states S_1 and S_2 differ only in location but not in orientation. The unit cell (heavily outlined small square) of the domain pair $\{\mathsf{S}_1, \mathsf{S}_2\}$ is identical with the unit cell of the tetragonal parent phase (*cf.* Fig. 3.4.2.5).

The two arrows attached to the circles in the domain pairs represent exaggerated displacements within the wall.

Domain pairs represent an intermediate step in analyzing microscopic structures of domain walls, as we shall see in Section 3.4.4.

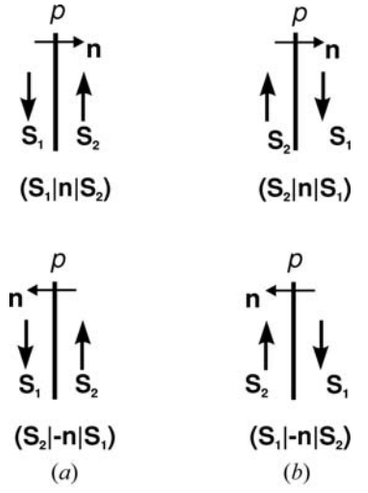

Fig. 3.4.4.1. Symbols of a simple twin. (*a*) Two different symbols with antiparallel normal **n**. (*b*) Symbols of the reversed twin.

3.4.4. Domain twins and domain walls

3.4.4.1. *Formal description of simple domain twins and planar domain walls of zero thickness*

In this section, we examine crystallographic properties of planar compatible domain walls and simple domain twins. The symmetry of these objects is described by layer groups. Since this concept is not yet common in crystallography, we briefly explain its meaning in Section 3.4.4.2. The exposition is performed in the continuum description, but most of the results apply with slight generalizations to the microscopic treatment that is illustrated with an example in Section 3.4.4.7.

We shall consider a *simple domain twin* $\mathbf{T}_{12}$ that consists of two domains $\mathbf{D}_1$ and $\mathbf{D}_2$ which meet along a planar domain wall $\mathbf{W}_{12}$ of zero thickness. Let us denote by p a *plane of the domain wall*, in brief *wall plane* of $\mathbf{W}_{12}$. This plane is specified by Miller indices (hkl), or by a normal **n** to the plane which also defines the sidedness (plus and minus side) of the plane p. By *orientation of the plane p* we shall understand a specification which can, but may not, include the sidedness of p. If both the orientation and the sidedness are given, then the plane p divides the space into two half-spaces. Using the bra–ket symbols, mentioned in Section 3.4.3.6, we shall denote by $(\,|$ the half-space on the negative side of p and by $|\,)$ the half-space on the positive side of p.

A *simple twin* consists of two (theoretically semi-infinite) domains $\mathbf{D}_1$ and $\mathbf{D}_2$ with domain states $\mathbf{S}_1$ and $\mathbf{S}_2$, respectively, that join along a planar domain wall the orientation of which is specified by the wall plane p with normal **n**. A symbol $(\mathbf{S}_1|\mathbf{n}|\mathbf{S}_2)$ specifies the domain twin unequivocally: domain $(\mathbf{S}_1|$, with domain region $(\,|$ filled with domain state $\mathbf{S}_1$, is on the negative side of p and domain $|\,\mathbf{S}_2)$ is on the positive side of p (see Fig. 3.4.4.1*a*).

If we were to choose the normal of opposite direction, *i.e.* $-\mathbf{n}$, the same twin would have the symbol $(\mathbf{S}_2|-\mathbf{n}|\mathbf{S}_1)$ (see Fig. 3.4.4.1*a*). Since these two symbols signify the same twin, we have the identity

$$(\mathbf{S}_1|\mathbf{n}|\mathbf{S}_2) \equiv (\mathbf{S}_2|-\mathbf{n}|\mathbf{S}_1). \qquad (3.4.4.1)$$

Thus, if we invert the normal $\mathbf{n}$ and simultaneously exchange domain states $\mathbf{S}_1$ and $\mathbf{S}_2$ in the twin symbol, we obtain an identical twin (see Fig. 3.4.4.1*a*). This identity expresses the fact that the specification of the twin by the symbol introduced above does not depend on the chosen direction of the wall normal $\mathbf{n}$.

The full symbol of the twin can be replaced by a shorter symbol $\mathbf{T}_{12}(\mathbf{n})$ if we accept a simple convention that the first lower index signifies the domain state that occupies the half space (| on the negative side of $\mathbf{n}$. Then the identity (3.4.4.1) in short symbols is

$$\mathbf{T}_{12}(\mathbf{n}) \equiv \mathbf{T}_{21}(-\mathbf{n}). \qquad (3.4.4.2)$$

If the orientation and sidedness of the plane p of a wall is known from the context or if it is not relevant, the specification of $\mathbf{n}$ in the symbol of the domain twin and domain wall can be omitted.

A twin $(\mathbf{S}_1|\mathbf{n}|\mathbf{S}_2)$, or $\mathbf{T}_{12}(\mathbf{n})$, can be formed by sectioning the ordered domain pair $(\mathbf{S}_1, \mathbf{S}_2)$ by a plane p with normal $\mathbf{n}$ and removing the domain state $\mathbf{S}_2$ on the negative side and domain state $\mathbf{S}_2$ on the positive side of the normal $\mathbf{n}$. This is the same procedure that is used in bicrystallography when an ideal bicrystal is derived from a dichromatic complex (see Section 3.2.2).

A twin with reversed order of domain states is called a *reversed twin*. The symbol of the twin reversed to the initial twin $(\mathbf{S}_1|\mathbf{n}|\mathbf{S}_2)$ is

$$(\mathbf{S}_2|\mathbf{n}|\mathbf{S}_1) \equiv (\mathbf{S}_1|-\mathbf{n}|\mathbf{S}_2) \qquad (3.4.4.3)$$

or

$$\mathbf{T}_{21}(\mathbf{n}) \equiv \mathbf{T}_{12}(-\mathbf{n}). \qquad (3.4.4.4)$$

A reversed twin $(\mathbf{S}_2|\mathbf{n}|\mathbf{S}_1) \equiv (\mathbf{S}_1|-\mathbf{n}|\mathbf{S}_2)$ is depicted in Fig. 3.4.4.1(*b*).

A *planar domain wall* is the interface between the domains $\mathbf{D}_1$ and $\mathbf{D}_2$ of the associated simple twin. Even a domain wall of zero thickness is specified not only by its orientation in space but also by the domain states that adhere to the minus and plus sides of the wall plane p. The symbol for the wall is, therefore, analogous to that of the twin, only in the explicit symbol the brackets ( ) are replaced by square brackets [ ] and $\mathbf{T}$ in the short symbol is replaced by $\mathbf{W}$:

$$[\mathbf{S}_1|\mathbf{n}|\mathbf{S}_2] \equiv [\mathbf{S}_2|-\mathbf{n}|\mathbf{S}_1] \qquad (3.4.4.5)$$

or by a shorter equivalent symbol

$$\mathbf{W}_{12}(\mathbf{n}) \equiv \mathbf{W}_{21}(-\mathbf{n}). \qquad (3.4.4.6)$$

3.4.4.2. *Layer groups*

An adequate concept for characterizing symmetry properties of simple domain twins and planar domain walls is that of layer groups. A layer group describes the symmetry of objects that exist in a three-dimensional space and have two-dimensional translation symmetry. Typical examples are two-dimensional planes in three-dimensional space [two-sided planes and sectional layer groups (Holser, 1958*a*,*b*), domain walls and interfaces of zero thickness], layers of finite thickness (*e.g.* domain walls and interfaces of finite thickness) and two semi-infinite crystals joined along a planar and coherent (compatible) interface [*e.g.* simple domain twins with a compatible (coherent) domain wall, bicrystals].

Table 3.4.4.1. *Crystallographic layer groups with continuous translations*

International	Non-coordinate
1	1
$\bar{1}$	$\underline{\bar{1}}$
112	2
11m	$\underline{m}$
112/m	2/$\underline{m}$
211	$\underline{2}$
m11	$\underline{m}$
2/m11	$\underline{2}/m$
222	$\underline{2}2\underline{2}$
mm2	mm2
m2m	$m\underline{2}\underline{m}$
mmm	$mm\underline{m}$
4	4
$\bar{4}$	$\underline{\bar{4}}$
4/m	4/$\underline{m}$
422	4$\underline{2}\underline{2}$
4mm	4mm
$\bar{4}$2m	$\underline{\bar{4}}\underline{2}m$
4/mmm	4/$\underline{m}mm$
3	3
$\bar{3}$	$\underline{\bar{3}}$
32	3$\underline{2}$
3m	3m
$\bar{3}m$	$\underline{\bar{3}}m$
6	6
$\bar{6}$	$\underline{\bar{6}}$
6/m	6/$\underline{m}$
622	6$\underline{2}\underline{2}$
6mm	6mm
$\bar{6}m$2	$\underline{\bar{6}}m\underline{2}$
6/mmm	6/$\underline{m}mm$

A *crystallographic layer group* comprises symmetry operations (isometries) that leave invariant a chosen crystallographic plane p in a crystalline object. There are two types of such operations:

(i) *side-preserving operations* keep invariant the normal $\mathbf{n}$ of the plane p, *i.e.* map each side of the plane p onto the same side. This type includes translations (discrete or continuous) in the plane p, rotations of $360^\circ/n$, $n = 2, 3, 4, 6$, around axes perpendicular to the plane p, reflections through planes perpendicular to p and glide reflections through planes perpendicular to p with glide vectors parallel to p. The corresponding symmetry elements are not related to the location of the plane p in space, *i.e.* they are the same for all planes parallel to p.

(ii) *side-reversing operations* invert the normal $\mathbf{n}$ of the plane *i.e.* exchange sides of the plane. Operations of this type are: an inversion through a point in the plane p, rotations of $360^\circ/n$, $n = 3, 4, 6$ around axes perpendicular to the plane followed by inversion through this point, 180° rotation and 180° screw rotation around an axis in the plane p, reflection and glide reflections through the plane p, and combinations of these operations with translations in the plane p. All corresponding symmetry elements are located in the plane p.

A layer group $\mathcal{L}$ consists of two parts:

$$\mathcal{L} = \widehat{\mathcal{L}} \cup \underline{s}\widehat{\mathcal{L}}, \qquad (3.4.4.7)$$

where $\widehat{\mathcal{L}}$ is a subgroup of $\mathcal{L}$ that comprises all side-preserving operations of $\mathcal{L}$; this group is isomorphic to a plane group and is called a *trivial layer group* or a *face group*. An underlined character $\underline{s}$ denotes a side-reversing operation and the left coset $\underline{s}\widehat{\mathcal{L}}$ contains all side-reversing operations of $\mathcal{L}$. Since $\widehat{\mathcal{L}}$ is a halving subgroup, the layer group $\mathcal{L}$ can be treated as a dichromatic (black-and-white) group in which side-preserving operations are

colour-preserving operations and side-reversing operations are colour-exchanging operations.

There are 80 layer groups with discrete two-dimensional translation subgroups [for a detailed treatment see *IT* E (2002), or *e.g.* Vainshtein (1994), Shubnikov & Kopcik (1974), Holser (1958*a*)]. Equivalent names for these layer groups are *net groups* (Opechowski, 1986), *plane groups in three dimensions* (Grell *et al.*, 1989), *groups in a two-sided plane* (Holser, 1958*a*,*b*) and others.

To these layer groups there correspond 31 point groups that describe the symmetries of crystallographic objects with two-dimensional continuous translations. Holser (1958*b*) calls these groups *point groups in a two-sided plane*, Kopský (1993) coins the term *point-like layer groups*. We shall use the term 'layer groups' both for layer groups with discrete translations, used in a microscopic description, and for crystallographic 'point-like layer groups' with continuous translations in the continuum approach. The geometrical meaning of these groups is similar and most of the statements and formulae hold for both types of layer groups.

Crystallographic layer groups with a continuous translation group [point groups of two-sided plane (Holser, 1958*b*)] are listed in Table 3.4.4.1. The *international notation* corresponds to international symbols of layer groups with discrete translations; this notation is based on the Hermann–Mauguin (international) symbols of three-dimensional space groups, where the *c* direction is the direction of missing translations and the character '1' represents a symmetry direction in the plane with no associated symmetry element (see *IT* E, 2002).

In the *non-coordinate notation* (Janovec, 1981), side-reversing operations are underlined. Thus *e.g.* $\underline{2}$ denotes a 180° rotation around a twofold axis in the plane *p* and $\underline{m}$ a reflection through this plane, whereas 2 is a side-preserving 180° rotation around an axis perpendicular to the plane and *m* is a side-preserving reflection through a plane perpendicular to the plane *p*. With exception of $\underline{\bar{1}}$ and $\underline{2}$, the symbol of an operation specifies the orientation of the plane *p*. This notation allows one to signify layer groups with different orientations in one reference coordinate system. Another non-coordinate notation has been introduced by Shubnikov & Kopcik (1974).

If a crystal with point-group symmetry *G* is bisected by a crystallographic plane *p*, then all operations of *G* that leave the plane *p* invariant form a *sectional layer group* = $\overline{\mathsf{G}(p)}$ *of the plane p in G*. Operations of the group $\overline{\mathsf{G}(p)}$ can be divided into two sets [see equation (3.4.4.7)]:

$$\overline{\mathsf{G}(p)} = \widehat{\mathsf{G}(p)} \cup \underline{g}\widehat{\mathsf{G}(p)}, \qquad (3.4.4.8)$$

where the trivial layer group $\widehat{\mathsf{G}(p)}$ expresses the symmetry of the crystal face with normal **n**. These face symmetries are listed in *IT* A (2002), Part 10, for all crystallographic point groups *G* and all orientations of the plane expressed by Miller indices (*hkl*). The underlined operation $\underline{g}$ is a side-reversing operation that inverts the normal **n**. The left coset $\underline{g}\widehat{\mathsf{G}(p)}$ contains all side-reversing operations of $\overline{\mathsf{G}(p)}$.

The number n_p of planes symmetrically equivalent (in *G*) with the plane *p* is equal to the index of $\overline{\mathsf{G}(p)}$ in *G*:

$$n_p = [G : \overline{\mathsf{G}(p)}] = |G| : |\overline{\mathsf{G}(p)}|. \qquad (3.4.4.9)$$

Example 3.4.4.1. As an example, we find the sectional layer group of the plane (010) in the group $G = 4_z/m_z m_x m_{xy}$ (see Fig. 3.4.2.2).

$$\begin{aligned} 4_z/m_z m_x m_{xy}(010) &= m_x 2_y m_z \cup \underline{m}_y\{m_x 2_y m_z\} \\ &= m_x 2_y m_z \cup \{\underline{m}_y, \underline{2}_z, \underline{\bar{1}}, \underline{2}_x\} \\ &= m_x \underline{m}_y m_z. \end{aligned} \qquad (3.4.4.10)$$

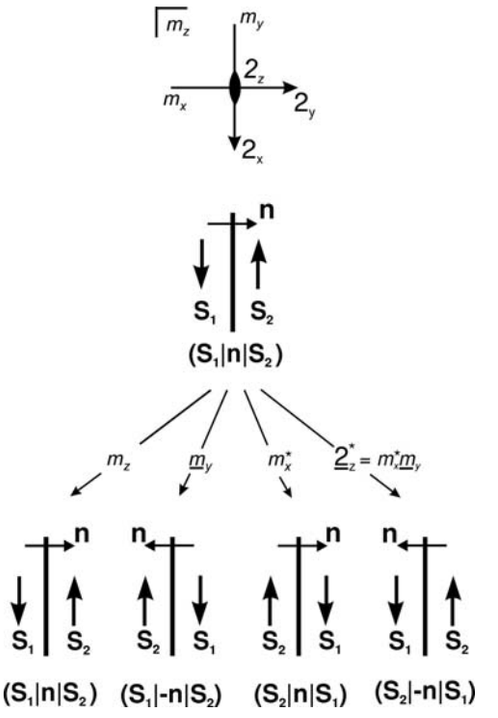

Fig. 3.4.4.2. A simple twin under the action of four types of operation that do not change the orientation of the wall plane *p*. Compare with Table 3.4.4.2.

In this example $n_p = |4_z/m_z m_x m_{xy}| : |m_x \underline{m}_y m_z| = 16 : 8 = 2$ and the plane crystallographically equivalent with the plane (010) is the plane (100) with sectional symmetry $\underline{m}_x m_y m_z$.

3.4.4.3. *Symmetry of simple twins and planar domain walls of zero thickness*

We shall examine the symmetry of a twin $(\mathbf{S}_1|\mathbf{n}|\mathbf{S}_j)$ with a planar zero-thickness domain wall with orientation and location defined by a plane *p* (Janovec, 1981; Zikmund, 1984; Zieliński, 1990). The symmetry properties of a planar domain wall $\mathbf{W}_{1j}$ are the same as those of the corresponding simple domain twin. Further, we shall consider twins but all statements also apply to the corresponding domain walls.

Operations that express symmetry properties of the twin must leave the orientation and location of the plane *p* invariant. We shall perform our considerations in the continuum description and shall assume that the plane *p* passes through the origin of the coordinate system. Then point-group symmetry operations leave the origin invariant and do not change the position of *p*.

If we apply an operation $g \in G$ to the twin $(\mathbf{S}_1|\mathbf{n}|\mathbf{S}_j)$, we get a crystallographically equivalent twin $(\mathbf{S}_i|\mathbf{n}_m|\mathbf{S}_k) \overset{G}{\sim} (\mathbf{S}_1|\mathbf{n}|\mathbf{S}_j)$ with other domain states and another orientation of the domain wall,

$$g(\mathbf{S}_1|\mathbf{n}|\mathbf{S}_j) = (g\mathbf{S}_1|g\mathbf{n}|g\mathbf{S}_j) = (\mathbf{S}_i|\mathbf{n}_m|\mathbf{S}_k), \quad g \in G. \qquad (3.4.4.11)$$

It can be shown that the transformation of a domain pair by an operation $g \in G$ defined by this relation fulfils the conditions of an action of the group *G* on a set of all domain pairs formed from the orbit $G\mathbf{S}_1$ (see Section 3.2.3.3). We can, therefore, use all concepts (stabilizer, orbit, class of equivalence *etc.*) introduced for domain states and also for domain pairs.

Operations *g* that describe symmetry properties of the twin $(\mathbf{S}_1|\mathbf{n}|\mathbf{S}_j)$ must not change the orientation of the wall plane *p* but can reverse the sides of *p*, and must either leave invariant both domain states $\mathbf{S}_1$ and $\mathbf{S}_j$ or exchange these two states. There are four types of such operations and their action is summarized in Table 3.4.4.2. It is instructive to follow this action in Fig. 3.4.4.2

Table 3.4.4.2. *Action of four types of operations g on a twin* $(\mathbf{S}_1|\mathbf{n}|\mathbf{S}_j)$

Operation g keeps the orientation of the plane p unchanged.

g	$g\mathbf{S}_1$	$g\mathbf{S}_j$	$g\mathbf{n}$	$g(\mathbf{S}_1\|$	$g\|\mathbf{S}_j)$	$g(\mathbf{S}_1\|\mathbf{n}\|\mathbf{S}_j) = (g\mathbf{S}_1\|g\mathbf{n}\|g\mathbf{S}_j)$	Resulting twin
f_{1j}	$\mathbf{S}_1$	$\mathbf{S}_j$	$\mathbf{n}$	$(\mathbf{S}_1\|$	$\|\mathbf{S}_j)$	$(\mathbf{S}_1\|\mathbf{n}\|\mathbf{S}_j)$	Initial twin
$\underline{s}_{1j}$	$\mathbf{S}_1$	$\mathbf{S}_j$	$-\mathbf{n}$	$\|\mathbf{S}_1)$	$(\mathbf{S}_j\|$	$(\mathbf{S}_1\|-\mathbf{n}\|\mathbf{S}_j) \equiv (\mathbf{S}_j\|\mathbf{n}\|\mathbf{S}_1)$	Reversed twin
$r^\star_{1j}$	$\mathbf{S}_j$	$\mathbf{S}_1$	$\mathbf{n}$	$(\mathbf{S}_j\|$	$\|\mathbf{S}_1)$	$(\mathbf{S}_j\|\mathbf{n}\|\mathbf{S}_1)$	Reversed twin
$\underline{t}^\star_{1j}$	$\mathbf{S}_j$	$\mathbf{S}_1$	$-\mathbf{n}$	$\|\mathbf{S}_j)$	$(\mathbf{S}_1\|$	$(\mathbf{S}_j\|-\mathbf{n}\|\mathbf{S}_1) \equiv (\mathbf{S}_1\|\mathbf{n}\|\mathbf{S}_j)$	Initial twin

using an example of the twin $(\mathbf{S}_1[010]\mathbf{S}_2)$ with domain states $\mathbf{S}_1$ and $\mathbf{S}_2$ from our illustrative example (see Fig. 3.4.2.2).

(1) An operation f_{1j} which leaves invariant the normal $\mathbf{n}$ and both domain states $\mathbf{S}_1$, $\mathbf{S}_j$ in the twin $(\mathbf{S}_1|\mathbf{n}|\mathbf{S}_j)$; such an operation does not change the twin and is called the *trivial symmetry operation of the twin*. An example of such an operation of the twin $(\mathbf{S}_1[010]\mathbf{S}_2)$ in Fig. 3.4.4.2 is the reflection m_z.

(2) An operation $\underline{s}_{1j}$ which inverts the normal $\mathbf{n}$ but leaves invariant both domain states $\mathbf{S}_1$ and $\mathbf{S}_j$. This *side-reversing* operation transforms the initial twin $(\mathbf{S}_1|\mathbf{n}|\mathbf{S}_j)$ into $(\mathbf{S}_1|-\mathbf{n}|\mathbf{S}_j)$, which is, according to (3.4.4.1), identical with the inverse twin $(\mathbf{S}_j|\mathbf{n}|\mathbf{S}_1)$. As in the non-coordinate notation of layer groups (see Table 3.4.4.1) we shall underline the side-reversing operations. The reflection $\underline{m}_y$ in Fig. 3.4.4.2 is an example of a side-reversing operation.

(3) An operation $r^\star_{1j}$ which exchanges domain states $\mathbf{S}_1$ and $\mathbf{S}_j$ but does not change the normal $\mathbf{n}$. This *state-exchanging operation*, denoted by a star symbol, transforms the initial twin $(\mathbf{S}_1|\mathbf{n}|\mathbf{S}_j)$ into a reversed twin $(\mathbf{S}_j|\mathbf{n}|\mathbf{S}_1)$. A state-exchanging operation in our example is the reflection $m^\star_x$.

(4) An operation $\underline{t}^\star_{1j}$ which inverts $\mathbf{n}$ and simultaneously exchanges $\mathbf{S}_1$ and $\mathbf{S}_j$. This operation, called the *non-trivial symmetry operation of a twin*, transforms the initial twin into $(\mathbf{S}_j|-\mathbf{n}|\mathbf{S}_1)$, which is, according to (3.4.4.1), identical with the initial twin $(\mathbf{S}_1|\mathbf{n}|\mathbf{S}_j)$. An operation of this type can be expressed as a product of a side-exchanging operation (underlined) and a state-exchanging operation (with a star), and will, therefore, be underlined and marked by a star. In Fig. 3.4.4.2, a non-trivial symmetry operation is for example the 180° rotation $\underline{2}^\star_z$.

We note that the star and the underlining do not represent any operation; they are just suitable auxiliary labels that can be omitted without changing the result of the operation.

To find all trivial symmetry operations of the twin $(\mathbf{S}_1|\mathbf{n}|\mathbf{S}_j)$, we recall that all symmetry operations that leave both $\mathbf{S}_1$ and $\mathbf{S}_j$ invariant constitute the symmetry group F_{1j} of the ordered domain pair $(\mathbf{S}_1, \mathbf{S}_j)$, $F_{1j} = F_1 \cap F_j$, where F_1 and F_j are the symmetry groups of $\mathbf{S}_1$ and $\mathbf{S}_j$, respectively. The sectional layer group of the plane p in group F_{1j} is (if we omit p)

$$\overline{\mathsf{F}}_{1j} = \widehat{\mathsf{F}}_{1j} \cup \underline{s}_{1j}\widehat{\mathsf{F}}_{1j}. \qquad (3.4.4.12)$$

The trivial (side-preserving) subgroup $\widehat{\mathsf{F}}_{1j}$ assembles all trivial symmetry operations of the twin $(\mathbf{S}_1|\mathbf{n}|\mathbf{S}_j)$. The left coset $\underline{s}_{1j}\widehat{\mathsf{F}}_{1j}$, where $\underline{s}_{1j}$ is a side-reversing operation, contains all side-reversing operations of this twin. In our example $\widehat{F}_{12} = \{1, m_z\}$ and $\underline{s}_{1j}\widehat{\mathsf{F}}_{1j} = \underline{m}_y\{1, m_z\} = \{\underline{m}_y, \underline{2}_x\}$ (see Fig. 3.4.4.2).

Similarly, the left coset $r^\star_{1j}\widehat{\mathsf{F}}_{1j}$ contains all state-exchanging operations, and $\underline{t}^\star_{1j}\widehat{\mathsf{F}}_{1j}$ all non-trivial symmetry operations of the twin $(\mathbf{S}_1|\mathbf{n}|\mathbf{S}_j)$. In the illustrative example, $r^\star_{1j}\widehat{\mathsf{F}}_{1j} = m^\star_x\{1, m_z\} = \{m^\star_x, 2^\star_y\}$ and $\underline{t}^\star_{1j}\widehat{\mathsf{F}}_{1j} = \underline{2}^\star_z\{1, m_z\} = \{\underline{2}^\star_z, \underline{\bar{1}}^\star\}$.

The trivial group $\widehat{F}_{1j}$ and its three cosets constitute the sectional layer group $\overline{J}_{1j}$ of the plane p in the symmetry group $J_{1j} = F_{1j} \cup g^\star_{1j}F_{1j}$ of the unordered domain pair $\{\mathbf{S}_1, \mathbf{S}_j\}$,

$$\overline{\mathsf{J}}_{1j} = \widehat{\mathsf{J}}_{1j} \cup \underline{s}_{1j}\widehat{\mathsf{J}}_{1j} = \widehat{\mathsf{F}}_{1j} \cup r^\star_{1j}\widehat{\mathsf{F}}_{1j} \cup \underline{s}_{1j}\widehat{\mathsf{F}}_{1j} \cup \underline{t}^\star_{1j}\widehat{\mathsf{F}}_{1j}, \qquad (3.4.4.13)$$

where $r^\star_{1j}$ is an operation of the left coset $g^\star_{1j}F_{1j}$ that leaves the normal $\mathbf{n}$ invariant and $\underline{t}^*_{1j} = \underline{s}_{1j}r^\star_{1j}$.

Group $\overline{\mathsf{J}}_{1j}$ can be interpreted as a symmetry group of a *twin pair* $(\mathbf{S}_1, \mathbf{S}_j|\mathbf{n}|\mathbf{S}_j, \mathbf{S}_1)$ consisting of a domain twin $(\mathbf{S}_1|\mathbf{n}|\mathbf{S}_j)$ and a superposed reversed twin $(\mathbf{S}_j|\mathbf{n}|\mathbf{S}_1)$ with a common wall plane p. This construct is analogous to a domain pair (dichromatic complex in bicrystallography) in which two homogeneous domain states $\mathbf{S}_1$ and $\mathbf{S}_j$ are superposed (see Section 3.4.3.1). In the same way as the group J_{1j} of domain pair $\{\mathbf{S}_1, \mathbf{S}_j\}$ is divided into two cosets with different results of the action on this domain pair, the symmetry group $\overline{\mathsf{J}}_{1j}$ of the twin pair can be decomposed into four cosets (3.4.4.13), each of which acts on a domain twin $(\mathbf{S}_j|\mathbf{n}|\mathbf{S}_1)$ in a different way, as specified in Table 3.4.4.2.

We can associate with operations from each coset in (3.4.4.13) a label. If we denote operations from $\widehat{\mathsf{F}}_{1j}$ without a label by *e*, underlining by *a* and star by *b*, then the multiplication of labels is expressed by the relations

$$a^2 = b^2 = e, \quad ab = ba. \qquad (3.4.4.14)$$

The four different labels *e*, *a*, *b*, *ab* can be formally viewed as four colours, the permutation of which is defined by relations (3.4.3.14); then the group $\overline{\mathsf{J}}_{1j}$ can be treated as a four-colour layer group.

Since the symbol of a point group consists of generators from which any operation of the group can be derived by multiplication, one can derive from the international symbol of a sectional layer group, in which generators are supplied with adequate labels, the coset decomposition (3.4.4.13).

Thus for the domain pair $\{\mathbf{S}_1, \mathbf{S}_2\}$ in Fig. 3.4.4.2 with $J^\star_{12} = m^\star_x m_y m_z$ [see equation (3.4.3.18)] and $p(010)$ we get the sectional layer group $\overline{\mathsf{J}}_{12}(010) = m^\star_x\underline{m}_y m_z$. Operations of this group (besides generators) are $m^\star_x\underline{m}_y = \underline{2}^\star_z$, $\underline{m}_y m_z = \underline{2}_x$, $m^\star_x m_z = 2^\star_y$, $m^\star_x\underline{2}_x = \underline{\bar{1}}^\star$.

All operations $g \in G$ that transform a twin into itself constitute the *symmetry group* $\mathsf{T}_{1j}(\mathbf{n})$ (or in short T_{1j}) *of the twin* $(\mathbf{S}_1|\mathbf{n}|\mathbf{S}_j)$. This is a layer group consisting of two parts:

$$\mathsf{T}_{1j} = \widehat{\mathsf{F}}_{1j} \cup \underline{t}^\star_{1j}\widehat{\mathsf{F}}_{1j}, \qquad (3.4.4.15)$$

where $\widehat{\mathsf{F}}_{1j}$ is a face group comprising all trivial symmetry operations of the twin and the left coset $\underline{t}^*_{1j}\widehat{\mathsf{F}}_{1j}$ contains all non-trivial operations of the twin that reverse the sides of the wall plane p and simultaneously exchange the states ($\mathbf{S}_1$ and $\mathbf{S}_j$).

One can easily verify that the symmetry $\mathsf{T}_{1j}(\mathbf{n})$ of the twin $(\mathbf{S}_1|\mathbf{n}|\mathbf{S}_j)$ is equal to the symmetry $\mathsf{T}_{j1}(\mathbf{n})$ of the reversed twin $(\mathbf{S}_j|\mathbf{n}|\mathbf{S}_1)$,

$$\mathsf{T}_{1j}(\mathbf{n}) = \mathsf{T}_{j1}(\mathbf{n}). \qquad (3.4.4.16)$$

Similarly, for sectional layer groups,

$$\overline{\mathsf{F}}_{1j}(\mathbf{n}) = \overline{\mathsf{F}}_{j1}(\mathbf{n}) \quad \text{and} \quad \overline{\mathsf{J}}_{1j}(\mathbf{n}) = \overline{\mathsf{J}}_{j1}(\mathbf{n}). \qquad (3.4.4.17)$$

Therefore, the symmetry of a twin $\mathsf{T}_{1j}(p)$ and of sectional layer groups $\overline{\mathsf{F}}_{1j}(p)$, $\overline{\mathsf{J}}_{1j}(p)$ is specified by the orientation of the plane p [expressed *e.g.* by Miller indices (hkl)] and not by the sidedness of p. However, the two layer groups $\overline{\mathsf{F}}_{1j}(p)$ and $\overline{\mathsf{F}}_{j1}(p)$, and $\mathsf{T}_{1j}(p)$ and $\mathsf{T}_{j1}(p)$ express the symmetry of *two different* objects, which can in special cases (non-transposable pairs and irreversible twins) be symmetrically non-equivalent.

The symmetry $\mathsf{T}_{1j}(\mathbf{n})$ also expresses the symmetry of the wall $\mathbf{W}_{1j}(\mathbf{n})$. This symmetry imposes constraints on the form of tensors

Table 3.4.4.3. *Classification of domain walls and simple twins*

T_{1j}	$\overline{\mathsf{J}}_{1j}$	Classification	Symbol
$\widehat{\mathsf{F}}_{1j} \cup \underline{t}^*_{1j}\widehat{\mathsf{F}}_{1j}$	$\widehat{\mathsf{F}}_{1j} \cup \underline{t}^*_{1j}\widehat{\mathsf{F}}_{1j} \cup r^*_{1j}\widehat{\mathsf{F}}_{1j} \cup \underline{s}_{1j}\widehat{\mathsf{F}}_{1j}$	Symmetric reversible	SR
$\widehat{\mathsf{F}}_{1j} \cup \underline{t}^*_{1j}\widehat{\mathsf{F}}_{1j}$	$\widehat{\mathsf{F}}_{1j} \cup \underline{t}^*_{1j}\widehat{\mathsf{F}}_{1j}$	Symmetric irreversible	SI
$\widehat{\mathsf{F}}_{1j}$	$\widehat{\mathsf{F}}_{1j} \cup \underline{s}_{1j}\widehat{\mathsf{F}}_{1j}$	Asymmetric side-reversible	A$\underline{\mathrm{R}}$
$\widehat{\mathsf{F}}_{1j}$	$\widehat{\mathsf{F}}_{1j} \cup r^*_{1j}\widehat{\mathsf{F}}_{1j}$	Asymmetric state-reversible	AR*
$\widehat{\mathsf{F}}_{1j}$	$\widehat{\mathsf{F}}_{1j}$	Asymmetric irreversible	AI

describing the properties of walls. In this way, the appearance of spontaneous polarization in domain walls has been examined (Přívratská & Janovec, 1999; Přívratská *et al.*, 2000).

According to their symmetry, twins and walls can be divided into two types: For a *symmetric twin (domain wall)*, there exists a non-trivial symmetry operation $\underline{t}^\star_{1j}$ and its symmetry is expressed by equation (3.4.4.15). A symmetric twin can be formed only from transposable domain pairs.

For an *asymmetric twin (domain wall)*, there is no non-trivial symmetry operation and its symmetry group is, therefore, confined to trivial group $\widehat{\mathsf{F}}_{1j}$,

$$\mathsf{T}_{1j} = \widehat{\mathsf{F}}_{1j}. \tag{3.4.4.18}$$

The difference between symmetric and asymmetric walls can be visualized in domain walls of finite thickness treated in Section 3.4.4.6.

The symmetry T_{1j} of a symmetric twin (wall), expressed by relation (3.4.4.15), is a layer group but not a sectional layer group of any point group. It can, however, be derived from the sectional layer group $\overline{\mathsf{F}}_{1j}$ of the corresponding ordered domain pair $(\mathbf{S}_1, \mathbf{S}_j)$ [see equation (3.4.4.12)] and the sectional layer group $\overline{\mathsf{J}}_{1j}$ of the unordered domain pair $\{\mathbf{S}_1, \mathbf{S}_j\}$ [see equation (3.4.4.13)],

$$\mathsf{T}_{1j} = \overline{\mathsf{J}}_{1j} - \{\overline{\mathsf{F}}_{1j} - \widehat{\mathsf{F}}_{1j}\} - \{\widehat{\mathsf{J}}_{1j} - \widehat{\mathsf{F}}_{1j}\}. \tag{3.4.4.19}$$

This is particularly useful in the microscopic description, since sectional layer groups of crystallographic planes in three-dimensional space groups are tabulated in *IT* E (2002), where one also finds an example of the derivation of the twin symmetry in the microscopic description.

The treatment of twin (wall) symmetry based on the concept of domain pairs and sectional layer groups of these pairs (Janovec, 1981; Zikmund, 1984) is analogous to the procedure used in treating interfaces in bicrystals (see Section 3.2.2; Pond & Bollmann, 1979; Pond & Vlachavas, 1983; Kalonji, 1985; Sutton & Balluffi, 1995). There is the following correspondence between terms: domain pair $\rightarrow$ dichromatic complex; domain wall $\rightarrow$ interface; domain twin with zero-thickness domain wall $\rightarrow$ ideal bicrystal; domain twin with finite-thickness domain wall $\rightarrow$ real (relaxed) bicrystal. Terms used in bicrystallography cover more general situations than domain structures (*e.g.* grain boundaries of crystals with non-crystallographic relations, phase interfaces). On the other hand, the existence of a high-symmetry phase, which is missing in bicrystallography, enables a more detailed discussion of crystallographically equivalent variants (orbits) of various objects in domain structures.

The symmetry group T_{1j} is the stabilizer of a domain twin (wall) in a certain group, and as such determines a class (orbit) of domain twins (walls) that are crystallographically equivalent with this twin (wall). The number of crystallographically equivalent twins is equal to the number of left cosets (index) of T_{1j} in the corresponding group. Thus the number $n_{W(p)}$ of equivalent domain twins (walls) with the same orientation defined by a plane p of the wall is

$$n_{W(p)} = [\overline{G(p)} : \mathsf{T}_{1j}] = |\overline{G(p)}| : |\mathsf{T}_{1j}|, \tag{3.4.4.20}$$

where $\overline{G(p)}$ is a sectional layer group of the plane p in the parent group G, $[\overline{G(p)} : \mathsf{T}_{1j}]$ is the index of T_{1j} in $\overline{G(p)}$ and absolute value denotes the number of operations in a group.

The set of all domain walls (twins) crystallographically equivalent in G with a given wall $[\mathbf{S}_1|\mathbf{n}|\mathbf{S}_j]$ forms a G-orbit of walls, $G\mathsf{W}_{1j} \equiv G[\mathbf{S}_1|\mathbf{n}|\mathbf{S}_j]$. The number n_W of walls in this G-orbit is

$$\begin{aligned} n_W &= [G : \mathsf{T}_{1j}] = |G| : |\mathsf{T}_{1j}| = (|G| : |\overline{G(p)}|)(|\overline{G(p)}| : |\mathsf{T}_{1j}|) \\ &= n_p n_{W(p)}, \end{aligned} \tag{3.4.4.21}$$

where n_p is the number of planes equivalent with plane p expressed by equation (3.4.4.9) and $n_{W(p)}$ is the number of equivalent domain walls with the plane p [see equation (3.4.4.20)]. Walls in one orbit have the same scalar properties (*e.g.* energy) and their structure and tensor properties are related by operations that relate walls from the same orbit.

Another aspect that characterizes twins and domain walls is the relation between a twin and the reversed twin. A twin (wall) which is crystallographically equivalent with the reversed twin (wall) will be called a *reversible twin (wall)*. If a twin and the reversed twin are not crystallographically equivalent, the twin will be called an *irreversible twin (wall)*. If a domain wall is reversible, then the properties of the reversed wall are fully specified by the properties of the initial wall, for example, these two walls have the same energy and their structures and properties are mutually related by a crystallographic operation. For irreversible walls, no relation exists between a wall and the reversed wall. Common examples of irreversible walls are electrically charged ferroelectric walls (walls carrying a nonzero polarization charge) and domain walls or discommensurations in phases with incommensurate structures.

A necessary and sufficient condition for reversibility is the existence of side-reversing and/or state-exchanging operations in the sectional layer group $\overline{\mathsf{J}}_{1j}$ of the unordered domain pair $\{\mathbf{S}_1, \mathbf{S}_j\}$ [see equation (3.4.4.13)]. This group also contains the symmetry group T_{1j} of the twin [see equation (3.4.4.15)] and thus provides a full symmetry characteristic of twins and walls,

$$\overline{\mathsf{J}}_{1j} = \mathsf{T}_{1j} \cup \underline{s}_{1j}\widehat{\mathsf{F}}_{1j} \cup \underline{t}^\star_{1j}\widehat{\mathsf{F}}_{1j}. \tag{3.4.4.22}$$

Sequences of walls and reversed walls appear in simple lamellar domain structures which are formed by domains with two alternating domain states, say $\mathbf{S}_1$ and $\mathbf{S}_2$, and parallel walls W_{12} and reversed walls W_{21} (see Fig. 3.4.2.1).

The distinction 'symmetric–asymmetric' and 'reversible–irreversible' provides a natural classification of domain walls and simple twins. *Five prototypes of domain twins and domain walls*, listed in Table 3.4.4.3, correspond to five subgroups of the sectional layer group $\overline{\mathsf{J}}_{1j}$: the sectional layer group $\overline{\mathsf{J}}_{1j}$ itself, the layer group of the twin $\mathsf{T}_{1j} = \widehat{\mathsf{F}}_{1j} \cup \underline{t}^*_{1j}\widehat{\mathsf{F}}_{1j}$, the sectional layer group $\overline{\mathsf{F}}_{1j} = \widehat{\mathsf{F}}_{1j} \cup \underline{s}_{1j}\widehat{\mathsf{F}}_{1j}$, the trivial layer group $\widehat{\mathsf{J}}_{1j} = \widehat{\mathsf{F}}_{1j} \cup r^*_{1j}\widehat{\mathsf{F}}_{1j}$ and the trivial layer group $\widehat{\mathsf{F}}_{1j}$.

An example of a symmetric reversible (SR) twin (and wall) is the twin $(\mathbf{S}_1[010]\mathbf{S}_2)$ in Fig. 3.4.4.2 with a non-trivial twinning operation $\underline{2}^\star_z$ and with reversing operations $\underline{m}_y$ and $m^\star_x$. The twin $(\mathbf{S}_1^+[\bar{1}10]\mathbf{S}_3^-)$ and reversed twin $(\mathbf{S}_3^-[\bar{1}10]\mathbf{S}_1^+)$ in Fig. 3.4.3.8 are symmetric and irreversible (SI) twins with a twinning operation

Table 3.4.4.4. *Symmetries of non-ferroelastic domain twins and walls*

T_{1j}	$\overline{\mathsf{J}}_{1j}$	Classification
1	1	AI
1	$\underline{\bar{1}}$	A$\underline{\text{R}}$
	$\underline{2}$	A$\underline{\text{R}}$
	$2^\star$	AR*
	$m^\star$	AR*
$\bar{1}^\star$	$\bar{1}^\star$	SI
	$\underline{2}/m^\star$	SR
	$2^\star/\underline{m}$	SR
2	$2m^\star m^\star$	AR*
$\underline{2}^\star$	$\underline{2}^\star$	SI
	$\underline{2}^\star/m^\star$	SR
	$2^\star\underline{2}^\star\underline{2}$	SR
	$\underline{2}^\star\underline{m}m^\star$	SR
m	m	AI
	$\underline{2}/m$	A$\underline{\text{R}}$
	$2^\star mm^\star$	AR*
$\underline{m}^\star$	$\underline{m}^\star$	SI
	$2^\star/\underline{m}^\star$	SR
	$\underline{m}^\star m^\star\underline{2}$	SR
$\underline{2}^\star/m$	$\underline{2}^\star/m$	SI
	$m\underline{m}m^\star$	SR
$2/\underline{m}^\star$	$2/\underline{m}^\star$	SI
	$m^\star m^\star\underline{m}^\star$	SR
	$4^\star/\underline{m}^\star$	SR
$2\underline{2}^\star\underline{2}^\star$	$2\underline{2}^\star\underline{2}^\star$	SI
	$\underline{m}m^\star m^\star$	SR
	$4^\star\underline{2}\underline{2}^\star$	SR
	$\underline{\bar{4}}\underline{2}^\star m^\star$	SR
$\underline{m}^\star m\underline{2}^\star$	$\underline{m}^\star m\underline{2}^\star$	SI
	$\underline{m}^\star mm^\star$	SR
$mm\underline{m}^\star$	$mm\underline{m}^\star$	SI
	$4^\star/\underline{m}^\star m^\star m$	SR
4	$4m^\star m^\star$	AR*
$\underline{\bar{4}}^\star$	$\underline{\bar{4}}^\star\underline{2}m^\star$	SR
$4/\underline{m}^\star$	$4/\underline{m}^\star$	SI
	$4/\underline{m}^\star m^\star m^\star$	SR
$4\underline{2}^\star\underline{2}^\star$	$4\underline{2}^\star\underline{2}^\star$	SI
	$4/\underline{m}m^\star m^\star$	SR
$\underline{\bar{4}}^\star\underline{2}^\star m$	$4^\star/\underline{m}m^\star m$	SR
$4/\underline{m}^\star mm$	$4/\underline{m}^\star mm$	SI
3	$3m^\star$	AR*
	$6^\star$	AR*
$\underline{\bar{3}}^\star$	$\underline{\bar{3}}^\star$	SI
	$\underline{\bar{3}}^\star m^\star$	SR
	$6^\star/\underline{m}$	SR
$3m$	$6^\star mm^\star$	AR*
$3\underline{2}^\star$	$3\underline{2}^\star$	SI
	$\underline{\bar{3}}m^\star$	SR
	$6^\star\underline{2}\underline{2}^\star$	SR
	$\underline{\bar{6}}\underline{2}^\star m^\star$	SR
$\underline{\bar{3}}^\star m$	$\underline{\bar{3}}^\star m$	SI
	$6^\star/\underline{m}mm^\star$	SR
6	$6m^\star m^\star$	AR*
$\underline{\bar{6}}^\star$	$\underline{\bar{6}}^\star$	SI
	$6^\star/\underline{m}^\star$	SR
	$\underline{\bar{6}}^\star\underline{2}m^\star$	SR
$6/\underline{m}^\star$	$6/\underline{m}^\star$	SI
	$6/\underline{m}^\star m^\star m^\star$	SR
$6\underline{2}^\star\underline{2}^\star$	$6\underline{2}^\star\underline{2}^\star$	SI
	$6/\underline{m}m^\star m^\star$	SR
$\underline{\bar{6}}^\star m\underline{2}^\star$	$\underline{\bar{6}}^\star m\underline{2}^\star$	SI
	$6^\star/\underline{m}^\star mm^\star$	SR
$6/\underline{m}^\star mm$	$6/\underline{m}^\star mm$	SI

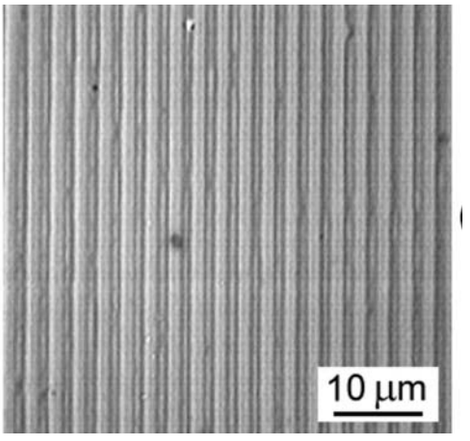

Fig. 3.4.4.3. Engineered periodic non-ferroelastic ferroelectric stripe domain structure within a lithium tantalate crystal with symmetry descent $\bar{6} \supset 3$. The domain structure is revealed by etching and observed in an optical microscope (Shur *et al.*, 2001). Courtesy of Vl. Shur, Ural State University, Ekaterinburg.

$\underline{m}^\star_{xy}$; no reversing operations exist (walls are charged and charged walls are always irreversible, since a charge is invariant with respect to any transformation of the space). The twin ($\mathbf{S}_1^-[110]\mathbf{S}_3^+$) and reversed twin ($\mathbf{S}_3^+[110]\mathbf{S}_1^-$) in the same figure are asymmetric state-reversible twins with state-reversing operation $m^\star_{xy}$ and with no non-trivial twinning operation.

The same classification also applies to domain twins and walls in a microscopic description.

As in the preceding section, we shall now present separately the symmetries of non-ferroelastic simple domain twins ['twinning without a change of crystal shape (or form)'] and of ferroelastic simple domain twins ['twinning with a change of crystal shape (or form)'; Klassen-Neklyudova (1964), Indenbom (1982)].

3.4.4.4. *Non-ferroelastic domain twins and domain walls*

Compatibility conditions impose no restriction on the orientation of non-ferroelastic domain walls. Any of the non-ferroelastic domain pairs listed in Table 3.4.3.4 can be sectioned on any crystallographic plane p and the sectional group $\overline{\mathsf{J}}_{1j}$ specifies the symmetry properties of the corresponding twin and domain wall. The analysis can be confined to one representative orientation of each class of equivalent planes, but a listing of all possible cases is too voluminous for the present article. We give, therefore, in Table 3.4.4.4 only possible symmetries T_{1j} and $\overline{\mathsf{J}}_{1j}$ of non-ferroelastic domain twins and walls, together with their classification, without specifying the orientation of the wall plane p.

Non-ferroelastic domain walls are usually curved with a slight preference for certain orientations (see Figs. 3.4.1.5 and 3.4.3.3). Such shapes indicate a weak anisotropy of the wall energy σ, *i.e.* small changes of σ with the orientation of the wall. The situation is different in ferroelectric domain structures, where charged domain walls have higher energies than uncharged ones.

A small energetic anisotropy of non-ferroelastic domain walls is utilized in producing *tailored domain structures* (Newnham *et al.*, 1975). A required domain pattern in a non-ferroelastic ferroelectric crystal can be obtained by evaporating electrodes of a desired shape (*e.g.* stripes) onto a single-domain plate cut perpendicular to the spontaneous polarization $\mathbf{P}_0$. Subsequent poling by an electric field switches only regions below the electrodes and thus produces the desired antiparallel domain structure.

Periodically poled ferroelectric domain structures fabricated by this technique are used for example in quasi-phase-matching optical multipliers (see *e.g.* Shur *et al.*, 1999, 2001; Rosenman *et*

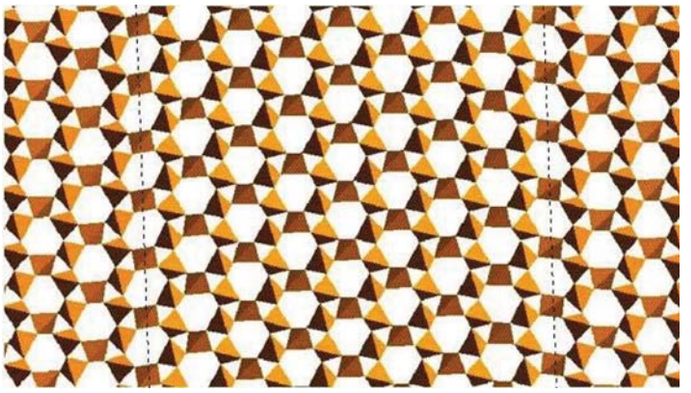

Fig. 3.4.4.4. Microscopic structure of two domain states and two parallel mutually reversed domain walls in the α phase of quartz. The left-hand vertical dotted line represents the domain wall W_{12}, the right-hand line is the reversed domain wall W_{12}. To the left of the left-hand line and to the right of the right-hand line are domains with domain state $\mathbf{S}_1$, the domain between the lines has domain state $\mathbf{S}_2$. For more details see text. Courtesy of M. Calleja, University of Cambridge.

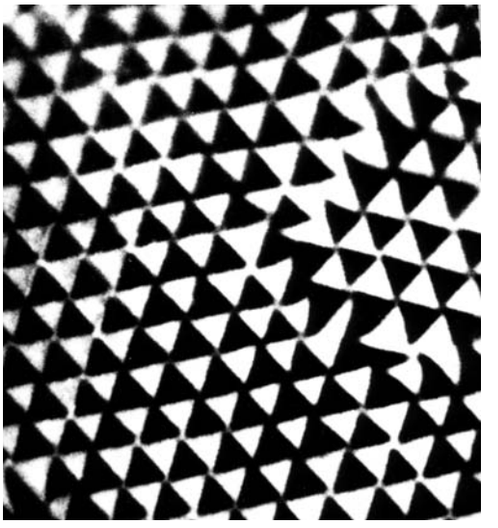

Fig. 3.4.4.5. Transmission electron microscopy (TEM) image of the incommensurate triangular ($3-q$ modulated) phase of quartz. The black and white triangles correspond to domains with domain states $\mathbf{S}_1$ and $\mathbf{S}_2$, and the transition regions between black and white areas to domain walls (discommensurations). For a domain wall of a certain orientation there are no reversed domain walls with the same orientation but reversed order of black and white; the walls are, therefore, non-reversible. Domain walls in regions with regular triangular structures are related by 120 and 240° rotations about the z direction and carry parallel spontaneous polarizations (see text). Triangular structures in two regions (blocks) with different orientations of the triangles are related *e.g.* by 2_x and carry, therefore, antiparallel spontaneous polarizations and behave macroscopically as two ferroelectric domains with antiparallel spontaneous polarization. Courtesy of E. Snoeck, CEMES, Toulouse and P. Saint-Grégoire, Université de Toulon.

al., 1998). An example of such an *engineered domain structure* is presented in Fig. 3.4.4.3.

Anisotropic domain walls can also appear if the Landau free energy contains a so-called Lifshitz invariant (see Section 3.1.3.3), which lowers the energy of walls with certain orientations and can be responsible for the appearance of an incommensurate phase (see *e.g.* Dolino, 1985; Tolédano & Tolédano, 1987; Tolédano & Dmitriev, 1996; Strukov & Levanyuk, 1998). The irreversible character of domain walls in a commensurate phase of crystals also containing (at least theoretically) an incommensurate phase has been confirmed in the frame of phenomenological theory by Ishibashi (1992). The incommensurate structure in quartz that demonstrates such an anisotropy is discussed at the end of the next example.

Example 3.4.4.2. Domain walls in α-phase of quartz. Quartz (SiO_2) undergoes a structural phase transition from the parent β phase (symmetry group $6_z2_x2_y$) to the ferroic α phase (symmetry 3_z2_x). The α phase can appear in two domain states $\mathbf{S}_1$ and $\mathbf{S}_2$, which have the same symmetry $F_1 = F_2 = 3_z2_x$. The symmetry J_{12} of the unordered domain pair $\{\mathbf{S}_1, \mathbf{S}_2\}$ is given by $J_{12}^\star = 3_z2_x \cup 2_y^*\{3_z2_x\} = 6_z^*2_x2_y^*$.

Table 3.4.4.5 summarizes the results of the symmetry analysis of domain walls (twins). Each row of the table contains data for one representative domain wall $\mathbf{W}_{12}(\mathbf{n}_{12})$ from one orbit $G\mathbf{W}_{12}(\mathbf{n}_{12})$. The first column of the table specifies the normal $\mathbf{n}$ of the wall plane p, further columns list the layer groups F_{12}, T_{12} and J_{12} that describe the symmetry properties and classification of the wall (defined in Table 3.4.4.3), and n_W is the number of symmetrically equivalent domain walls [*cf.* equation (3.4.4.21)].

The last two columns give possible components of the spontaneous polarization $\mathbf{P}$ of the wall $\mathbf{W}_{12}(\mathbf{n})$ and the reversed wall $\mathbf{W}_{21}(\mathbf{n})$. Except for walls with normals [001] and [100], all walls are polar, *i.e.* they can be spontaneously polarized. The reversal of the polarization in reversible domain walls requires the reversal of domain states. In irreversible domain walls, the reversal of $\mathbf{W}_{12}$ into $\mathbf{W}_{21}$ is accompanied by a change of the polarization $\mathbf{P}$ into $\mathbf{P}'$, which may have a different absolute value and direction different to that of $\mathbf{P}$.

The structure of two domain states and two mutually reversed domain walls obtained by molecular dynamics calculations are depicted in Fig. 3.4.4.4 (Calleja *et al.*, 2001). This shows a projection on the *ab* plane of the structure represented by SiO_4 tetrahedra, in which each tetrahedron shares four corners. The threefold symmetry axes in the centres of distorted hexagonal channels and three twofold symmetry axes (one with vertical orientation) perpendicular to the threefold axes can be easily seen. The two vertical dotted lines are the wall planes p of two mutually reversed walls $[\mathbf{S}_1[010]\mathbf{S}_2] = \mathbf{W}_{12}[010]$ and $[\mathbf{S}_2[010]\mathbf{S}_1] = \mathbf{W}_{21}[010]$. In Table 3.4.4.5 we find that these walls have the symmetry $\mathsf{T}_{12}[010] = \mathsf{T}_{21}[010] = \underline{2}_x2_y^\star\underline{2}_z^\star$, and in Fig. 3.4.4.4 we can verify that the operation $\underline{2}_x$ is a 'side-reversing' operation $\underline{s}_{12}$ of the wall (and the whole twin as wall), operation $2_y^\star$ is a 'state-exchanging operation' $r_{12}^\star$ and the operation $\underline{2}_z^\star$ is a non-trivial 'side-and-state reversing' operation $\underline{t}_{12}^\star$ of the wall. The walls

Table 3.4.4.5. *Symmetry properties of domain walls in quartz*

$|\mathbf{P}| \neq |\mathbf{P}'|,\ P'_\alpha \neq -P_\alpha,\ \alpha = x, y, z.$

n	$\widehat{\mathsf{F}}_{12}$	T_{12}	$\overline{\mathsf{J}}_{12}$	Classification	n_W	$\mathbf{P}(\mathbf{W}_{12})$	$\mathbf{P}(\mathbf{W}_{21})$
[001]	3_z	$3_z\underline{2}_y^*$	$6_z^*\underline{2}_x\underline{2}_y^*$	SR	2		
[100]	2_x	$2_x\underline{2}_y^*2_z^*$	$2_x\underline{2}_y^*\underline{2}_z^*$	SI	3		
[010]	1	$\underline{2}_z^*$	$\underline{2}_x2_y^*\underline{2}_z^*$	SR	6	$0, 0, P_z$	$0, 0, -P_z$
[0*vw*]	1	1	$\underline{2}_x$	A$\underline{\mathrm{R}}$	12	P_x, P_y, P_z	$P_x, -P_y, -P_z$
[*u*0*w*]	1	$\underline{2}_y^*$	$\underline{2}_y^*$	SI	6	$0, P_y, 0$	$0, -P'_y, 0$
[*uv*0]	1	$\underline{2}_z^*$	$\underline{2}_z^*$	SI	6	$0, 0, P_z$	$0, 0, P'_z$
[*uvw*]	1	1	1	AI	12	P_x, P_y, P_z	P'_x, P'_y, P'_z

Table 3.4.4.6. *Symmetry properties of ferroelastic domain twins and compatible domain walls*

T_{1j}	$\overline{\mathsf{J}}_{1j}$	Classification		$K_{1j}[F_1]$
1	$\underline{2}$	V	A$\underline{\mathrm{R}}$	$4^\star[2]$, $\bar{4}^\star[2]$, 6[2], $6/m[2]$
1	$\underline{2}$	V	A$\underline{\mathrm{R}}$	
1	$2^\star$	W	AR*	$2^\star[1]$, 422[2], $\bar{4}2m[m]$, 32[2], $\bar{3}m[m]$, 622[2], $\bar{6}m2[m]$, 432[222], $m\bar{3}m[mm2]$, $m\bar{3}m[2^\star_{xy}][mm2]$
$\underline{2}^\star$	$\underline{2}^\star$	V	SI	
1	$2^\star$	W	AR*	23[3], 432[4], 432[3], $m\bar{3}m[\bar{4}]$
$\underline{2}^\star$	$\underline{2}^\star$	W	SI	
1	$m^\star$	V	AR*	$m^\star[1]$, $4mm[m]$, $\bar{4}2m[2]$, $3m[m]$, $\bar{3}m[2]$, $6mm[m]$, $\bar{6}m2[2]$, $\bar{4}3m[mm2]$, $m\bar{3}m[222]$, $m\bar{3}m[m^\star_{xy}][m2m]$
$\underline{m}^\star$	$\underline{m}^\star$	W	SI	
1	$m^\star$	W	AR*	$m\bar{3}[3]$, $\bar{4}3m[\bar{4}]$, $\bar{4}3m[3]$, $m\bar{3}m[4]$
$\underline{m}^\star$	$\underline{2}^\star$	W	SI	
$\underline{2}^\star$	$2^\star\underline{2}^\star\underline{2}$	W	SR	$2^\star2^\star2[2]$, $4^\star22^\star[222]$, $\bar{4}^\star2^\star m[mm2]$, 622[222], $6/mmm[mm2]$, 432[422], 432[32], $m\bar{3}m[\bar{4}2m]$
$\underline{2}^\star$	$\underline{2}^\star2^\star\underline{2}$	W	SR	
$\underline{2}^\star$	$\underline{2}^\star/m^\star$	V	SR	$2^\star/m^\star[\bar{1}]$, $4/mmm[2/m]$, $\bar{3}m[2/m]$, $6/mmm[2/m]$, $m\bar{3}m[mmm]$
$\underline{m}^\star$	$2^\star/\underline{m}^\star$	W	SR	
$\underline{2}^\star$	$\underline{2}^\star/m^\star$	W	SR	$m\bar{3}[\bar{3}]$, $m\bar{3}m[4/m]$, $m\bar{3}m[\bar{3}]$
$\underline{m}^\star$	$2^\star/\underline{m}^\star$	W	SR	
m	m	V	AI	$4/m[m]$, $\bar{6}[m]$, $6/m[m]$
m	m	V	AI	
m	$\underline{2}/m$	V	A$\underline{\mathrm{R}}$	$4^\star/m[2/m]$, $6/m[2/m]$
m	$\underline{2}/m$	V	A$\underline{\mathrm{R}}$	
$\underline{m}^\star$	$m^\star\underline{m}^\star\underline{2}$	W	SR	$m^\star m^\star2[2]$, $4^\star mm^\star[mm\underline{2}]$, $\bar{4}^\star2m^\star[222]$, $6mm[mm2]$, $6/mmm[222]$, $\bar{4}3m[\bar{4}2m]$, $m\bar{3}m[422]$, $m\bar{3}m[32]$
$\underline{m}^\star$	$\underline{m}^\star m^\star\underline{2}$	W	SR	
m	$m^\star2^\star m$	W	AR*	$m^\star2^\star m[m]$, $4/mmm[2mm]$, $\bar{6}m2[m2m]$, $6/mmm[m2m]$, $\bar{4}3m[3m]$, $m\bar{3}m[4mm]$, $m\bar{3}m[\bar{4}2m]$, $m\bar{3}m[3m]$
$\underline{m}^\star\underline{2}^\star m$	$\underline{m}^\star\underline{2}^\star m$	W	SI	
$\underline{m}^\star\underline{2}^\star m$	$\underline{m}^\star m^\star m$	W	SR	$m^\star m^\star m[2/m]$, $4^\star/mmm^\star[mmm]$, $6/mmm[mmm]$, $m\bar{3}m[4/mmm]$, $m\bar{3}m[\bar{3}m]$
$2^\star\underline{m}^\star m$	$m^\star\underline{m}^\star m$	W	SR	

$\mathbf{W}_{12}[010]$ and $\mathbf{W}_{21}[010]$ are, therefore, symmetric and reversible walls.

During a small temperature interval above the appearance of the α phase at 846 K, there exists an incommensurate phase that can be treated as a regular domain structure, consisting of triangular columnar domains with domain walls (discommensurations) of negative wall energy σ (see *e.g.* Dolino, 1985). Both theoretical considerations and electron microscopy observations (see *e.g.* Van Landuyt *et al.*, 1985) show that the wall normal has the $[uv0]$ direction. From Table 3.4.4.5 it follows that there are six equivalent walls that are symmetric but irreversible, therefore any two equivalent walls differ in orientation.

This prediction is confirmed by electron microscopy in Fig. 3.4.4.5, where black and white triangles correspond to domains with domain states $\mathbf{S}_1$ and $\mathbf{S}_2$, and the transition regions between black and white areas to domain walls (discommensurations). To a domain wall of a certain orientation no reversible wall appears with the same orientation but with a reversed order of black and white. Domain walls in homogeneous triangular parts of the structure are related by 120 and 240° rotations and carry, therefore, parallel spontaneous polarizations; wall orientations in two differently oriented blocks (the middle of the right-hand part and the rest on the left-hand side) are related by 180° rotations about the axis 2_x in the plane of the photograph and are, therefore, polarized in antiparallel directions (for more details see Saint-Grégoire & Janovec, 1989; Snoeck *et al.*, 1994). After cooling down to room temperature, the wall energy becomes positive and the regular domain texture changes into a coarse domain structure in which these six symmetry-related wall orientations still prevail (Van Landuyt *et al.*, 1985).

3.4.4.5. *Ferroelastic domain twins and walls. Ferroelastic twin laws*

As explained in Section 3.4.3.6, from a domain pair $(\mathbf{S}_1, \mathbf{S}_j)$ of ferroelastic single-domain states with two perpendicular equally deformed planes p and p' one can form four different ferroelastic twins (see Fig. 3.4.3.8). Two mutually reversed twins $(\mathbf{S}_1|\mathbf{n}|\mathbf{S}_j)$ and $(\mathbf{S}_j|\mathbf{n}|\mathbf{S}_1)$ have the same twin symmetry $\mathsf{T}_{1j}(p)$ and the same symmetry $\overline{\mathsf{J}}_{1j}(p)$ of the twin pair $(\mathbf{S}_1, \mathbf{S}_j|\mathbf{n}|\mathbf{S}_j, \mathbf{S}_1)$. The *ferroelastic twin laws* can be expressed by the layer group $\mathsf{J}_{1j}(p)$ or, in a less complete way (without specification of reversibility), by the twin symmetry $\mathsf{T}_{1j}(p)$. The same holds for two mutually reversed twins $(\mathbf{S}_1|\mathbf{n}'|\mathbf{S}_j)$ and $(\mathbf{S}_j|\mathbf{n}'|\mathbf{S}_1)$ with a twin plane p' perpendicular to p.

Table 3.4.4.6 summarizes possible symmetries T_{1j} of ferroelastic domain twins and corresponding ferroelastic twin laws $\overline{\mathsf{J}}_{1j}$. Letters V and W signify strain-dependent and strain-independent (with a fixed orientation) domain walls, respectively. The classification of domain walls and twins is defined in Table 3.4.4.3. The last column contains twinning groups $K_{1j}[F_1]$ of ordered domain pairs $(\mathbf{S}_1, \mathbf{S}_j)$ from which these twins can be formed. The symbol of K_{1j} is followed by a symbol of the group F_1 given in square brackets. The twinning group $K_{1j}[F_1]$ specifies, up to two cases, a class of equivalent domain pairs [orbit $G(\mathbf{S}_1, \mathbf{S}_j)$] (see Section 3.4.3.4). More details on particular cases (orientation of domain walls, disorientation angle, twin axis) can be found in synoptic Table 3.4.3.6. From this table follow two general conclusions:

(1) All layer groups describing the symmetry of compatible ferroelastic domain walls are polar groups, therefore *all compatible ferroelastic domain walls in dielectric crystals can be spontaneously polarized*. The direction of the spontaneous polarization is parallel to the intersection of the wall plane p and the plane of shear (*i.e.* a plane perpendicular to the axis of the ferroelastic domain pair, see Fig. 3.4.3.5*b* and Section 3.4.3.6.2).

(2) *Domain twin* $(\mathbf{S}_1|\mathbf{n}|\mathbf{S}_j)$ *formed in the parent clamping approximation from a single-domain pair* $(\mathbf{S}_1, \mathbf{S}_j)$ *and the relaxed domain twin* $(\mathbf{S}_1^+|\mathbf{n}|\mathbf{S}_j^-)$ *with disoriented domain states have the same symmetry groups* T_{1j} and $\overline{\mathsf{J}}_{1j}$.

This follows from simple reasoning: all twin symmetries T_{1j} in Table 3.4.4.6 have been derived in the parent clamping approximation and are expressed by the orthorhombic group $mm2$ or by some of its subgroups. As shown in Section 3.4.3.6.2, the maximal symmetry of a mechanically twinned crystal is also $mm2$. An

additional simple shear accompanying the lifting of the parent clamping approximation cannot, therefore, decrease the symmetry $\mathsf{T}_{1j}(p)$ derived in the parent clamping approximation. In a similar way, one can prove the statement for the group $\overline{\mathsf{J}}_{1j}(p)$ of the twin pairs $(\mathbf{S}_1, \mathbf{S}_j|\mathbf{n}|\mathbf{S}_j, \mathbf{S}_1)$ and $(\mathbf{S}_1^+, \mathbf{S}_j^-|\mathbf{n}|\mathbf{S}_j^-, \mathbf{S}_1^+)$.

3.4.4.6. *Domain walls of finite thickness – continuous description*

A domain wall of zero thickness is a geometrical construct that enabled us to form a twin from a domain pair and to find a layer group that specifies the *maximal symmetry* of that twin. However, real domain walls have a finite, though small, thickness. Spatial changes of the structure within a wall may, or may not, lower the wall symmetry and can be conveniently described by a *phenomenological theory*.

We shall consider the simplest case of a one nonzero component η of the order parameter (see Section 3.1.2). Two nonzero equilibrium homogeneous values of $-\eta_0$ and $+\eta_0$ of this parameter correspond to two domain states $\mathbf{S}_1$ and $\mathbf{S}_2$. Spatial changes of the order parameter in a domain twin $(\mathbf{S}_1|\mathbf{n}|\mathbf{S}_2)$ with a zero-thickness domain wall are described by a step-like function $\eta(\xi) = -\eta_0$ for $\xi < 0$ and $\eta(\xi) = +\eta_0$ for $\xi > 0$, where ξ is the distance from the wall of zero thickness placed at $\xi = 0$.

A domain wall of finite thickness is described by a function $\eta(\xi)$ with limiting values $-\eta_0$ and η_0:

$$\lim_{\xi\to-\infty}\eta(\xi) = -\eta_0, \quad \lim_{\xi\to+\infty}\eta(\xi) = \eta_0. \tag{3.4.4.23}$$

If the wall is symmetric, then the profile $\eta(\xi)$ in one half-space, say $\xi < 0$, determines the profile in the other half-space $\xi > 0$. For continuous $\eta(\xi)$ fulfilling conditions (3.4.4.23) this leads to the condition

$$\eta(\xi) = -\eta(-\xi), \tag{3.4.4.24}$$

i.e. $\eta(\xi)$ must be an odd function. This requirement is fulfilled if there exists a non-trivial symmetry operation of a domain wall (twin): a side reversal $(\xi \to -\xi)$ combined with an exchange of domain states $[\eta(\xi) \to -\eta(\xi)]$ results in an identical wall profile.

A particular form of the wall profile $\eta(\xi)$ can be deduced from Landau theory. In the simplest case, the dependence $\eta(\xi)$ of the domain wall would minimize the free energy

$$\int_{-\infty}^{\infty}\left(\Phi_0 + \tfrac{1}{2}\alpha(T - T_c)\eta^2 + \tfrac{1}{4}\beta\eta^4 + \tfrac{1}{2}\delta\left(\tfrac{d^2\eta}{d\xi^2}\right)^2\right)\mathrm{d}\xi, \tag{3.4.4.25}$$

where α, β, δ are phenomenological coefficients and T and T_c are the temperature and the temperature of the phase transition, respectively. The first three terms correspond to the homogeneous part of the Landau free energy (see Section 3.2.1) and the last term expresses the energy of the spatially changing order parameter. This variational task with boundary conditions (3.4.4.23) has the following solution (see *e.g.* Salje, 1990, 2000*b*; Ishibashi, 1990; Strukov & Levanyuk, 1998)

$$\eta(\xi) = \eta_0 \tanh(\xi/w), \tag{3.4.4.26}$$

where the value w specifies one half of the *effective thickness* $2w$ *of the domain wall* and is given by

$$w = \sqrt{2\delta/\alpha(T_c - T)}. \tag{3.4.4.27}$$

This dependence, expressed in relative dimensionless variables ξ/w and η/η_0, is displayed in Fig. 3.4.4.6.

The wall profile $\eta(\xi)$ expressed by solution (3.4.4.26) is an odd function of ξ,

$$\eta(-\xi) = \eta_0 \tanh(-\xi/w) = -\eta_0 \tanh(\xi/w) = -\eta(\xi), \tag{3.4.4.28}$$

and fulfils thus the condition (3.4.4.24) of a symmetric wall.

The wall thickness can be estimated from electron microscopy observations, or more precisely by a diffuse X-ray scattering technique (Locherer *et al.*, 1998). The effective thickness $2w$ [see equation (3.4.4.26)] in units of crystallographic repetition length A normal to the wall ranges from $2w/A = 2$ to $2w/A = 12$, *i.e.* $2w$ is about 10–100 nm (Salje, 2000*b*). The temperature dependence of the domain wall thickness expressed by equation (3.4.4.27) has been experimentally verified, *e.g.* on $LaAlO_3$ (Chrosch & Salje, 1999).

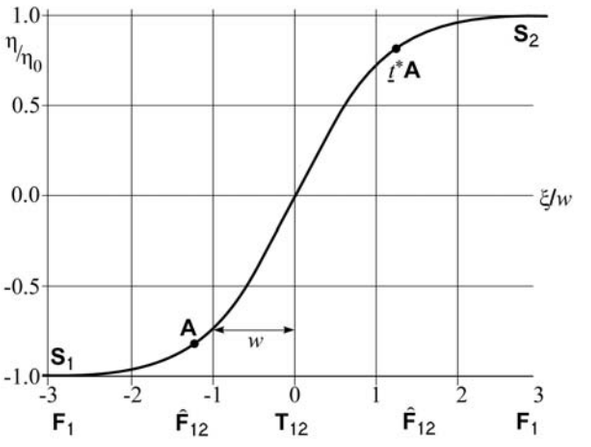

Fig. 3.4.4.6. Profile of the one-component order parameter $\eta(\xi)$ in a symmetric wall (S). The effective thickness of the wall is $2w$.

The energy σ of the domain wall per unit area equals the difference between the energy of the twin and the energy of the single-domain crystal. For a one nonzero component order parameter with the profile (3.4.4.26), the wall energy σ is given by (Strukov & Levanyuk, 1998)

$$\sigma = \int_{-\infty}^{\infty}\left[\Phi(\eta(\xi)) - \Phi(\eta_0)\right]\mathrm{d}\xi = \frac{2\sqrt{2\delta}}{3\beta}[\alpha(T_c - T)]^{3/2}, \tag{3.4.4.29}$$

where $2w$ is the effective thickness of the wall [see equation (3.4.4.27)] and the coefficients are defined in equation (3.4.4.25).

The order of magnitude of the wall energy σ of ferroelastic and non-ferroelastic domain walls is typically several millijoule per square metre (Salje, 2000*b*).

Example 3.4.4.3. In our example of a ferroelectric phase transition $4_z/m_z m_x m_{xy} \supset 2_x m_y m_z$, one can identify η with the P_1 component of spontaneous polarization and ξ with the axis y. One can verify in Fig. 3.4.4.6 that the symmetry $\mathsf{T}_{12}[010] = \underline{2}_z^\star/m_z$ of the twin $(\mathbf{S}_1[010]\mathbf{S}_2)$ with a zero-thickness domain wall is retained in the domain wall with symmetric profile (3.4.4.26): both non-trivial symmetry operations $\underline{2}_z^\star$ and $\underline{1}^\star$ transform the profile $\eta(y)$ into an identical function.

This example illustrates another feature of a symmetric wall: All non-trivial symmetry operations of the wall are located at the central plane $\xi = 0$ of the finite-thickness wall. The sectional group T_{12} of this plane thus expresses the *symmetry of the central layer* and also the *global symmetry* of a symmetric wall (twin). The *local symmetry* of the off-centre planes $\xi \neq 0$ is equal to the face group $\widehat{\mathsf{F}}_{12}$ of the the layer group T_{12} (in our example $\widehat{\mathsf{F}}_{12} = \{1, m_z\}$).

The relation between a wall profile $\eta(\xi)$ of a *symmetric reversible* (SR) *wall* and the profile $\eta^{\mathrm{rev}}(\xi)$ of the reversed wall is illustrated in Fig. 3.4.4.7, where the the dotted curve is the wall profile $\eta^{\mathrm{rev}}(\xi)$ of the reversed wall. The profile $\eta^{\mathrm{rev}}(\xi)$ of the reversed wall is completely determined by the the profile $\eta(\xi)$ of the initial wall, since both profiles are related by equations

$$\eta^{\mathrm{rev}}(\xi) = -\eta(\xi) = \eta(-\xi). \tag{3.4.4.30}$$

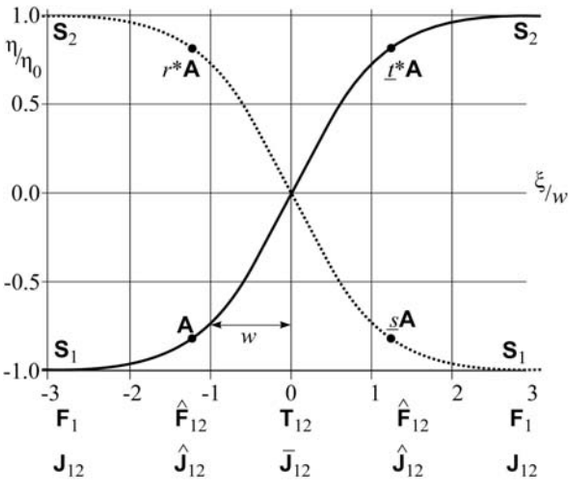

Fig. 3.4.4.7. Profiles of the one-component order parameter $\eta(\xi)$ in a symmetric wall (solid curve) and in the reversed wall (dotted curve). The wall is symmetric and reversible (SR).

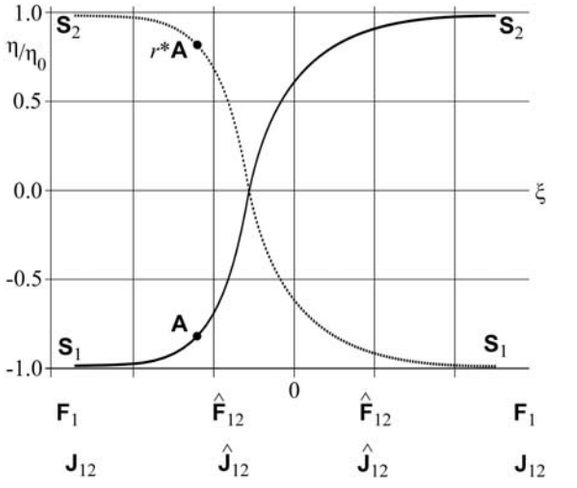

Fig. 3.4.4.8. Profiles of the one-component order parameter $\eta(\xi)$ in an asymmetric wall (solid curve) and in the reversed asymmetric wall (dotted curve). The wall is asymmetric and state-reversible (AR*).

The first part of the equation corresponds to a state-exchanging operation $r^{\star}_{12}$ (*cf.* point $r^{\star}$A in Fig. 3.4.4.7) and the second one to a side-reversing operation $\underline{s}_{12}$ (point $\underline{s}$A in the same figure). In a symmetric reversible wall, both types of reversing operations exist (see Table 3.4.4.3).

In a *symmetric irreversible* (SI) *wall* both initial and reversed wall profiles fulfil symmetry condition (3.4.4.24) but equations (3.4.4.30) relating both profiles do not exist. The profiles $\eta(\xi)$ and $\eta^{\rm rev}(\xi)$ may differ in shape and surface wall energy. Charged domain walls are always irreversible.

A possible profile of an *asymmetric domain wall* is depicted in Fig. 3.4.4.8 (full curve). There is no relation between the negative part $\eta(\xi) < 0$ and positive part $\eta(\xi) > 0$ of the wall profile $\eta(\xi)$. Owing to the absence of non-trivial twin operations, there is no central plane with higher symmetry. The local symmetry (sectional layer group) at any location ξ within the wall is equal to the face group $\widehat{\mathsf{F}}_{12}$. This is also the global symmetry T_{12} of the entire wall, $\mathsf{T}_{12} = \widehat{\mathsf{F}}_{12}$.

The dotted curve in Fig. 3.4.4.8 represents the reversed-wall profile of an *asymmetric state-reversible* (AR*) *wall* that is related to the initial wall by state-exchanging operations $r^{\star}_{12}\widehat{\mathsf{F}}_{12}$ (see Table 3.4.4.5),

$$\eta^{\rm rev}(\xi) = -\eta(\xi). \qquad (3.4.4.31)$$

An example of an *asymmetric side-reversible* (A$\underline{\rm R}$) *wall* is shown in Fig. 3.4.4.9. In this case, an asymmetric wall (full curve) and reversed wall (dotted curve) are related by side-reversing operations $\underline{s}_{12}\widehat{\mathsf{F}}_{12}$:

$$\eta^{\rm rev}(\xi) = \eta(-\xi). \qquad (3.4.4.32)$$

In an *asymmetric irreversible* (AI) *wall*, both profiles $\eta(\xi)$ and $\eta^{\rm rev}(\xi)$ are asymmetric and there is no relation between these two profiles.

The *symmetry* $\mathsf{T}_{12}(\eta)$ *of a finite-thickness wall* with a profile $\eta(\xi)$ is equal to or lower than the symmetry T_{12} of the corresponding zero-thickness domain wall, $\mathsf{T}_{12} \supseteq \mathsf{T}_{12}(\eta)$. A symmetry descent $\mathsf{T}_{12} \supset \mathsf{T}_{12}(\eta)$ can be treated as a phase transition in the domain wall (see *e.g.* Bul'bich & Gufan, 1989*a*,*b*; Sonin & Tagancev, 1989). There are $n_{W(\eta)}$ equivalent *structural variants of the finite-thickness domain wall* with the same orientation and the same energy but with different structures of the wall,

$$n_{W(\eta)} = [\mathsf{T}_{12} : \mathsf{T}_{12}(\eta)] = |\mathsf{T}_{12}| : |\mathsf{T}_{12}(\eta)|. \qquad (3.4.4.33)$$

Domain-wall variants – two-dimensional analogues of domain states – can coexist and meet along line defects – one-dimensional analogues of a domain wall (Tagancev & Sonin, 1989).

Symmetry descent in domain walls of finite thickness may occur if the order parameter η has more than one nonzero component. We can demonstrate this on ferroic phases with an order parameter with two components η_1 and η_2. The profiles $\eta_1(\xi)$ and $\eta_2(\xi)$ can be found, as for a one-component order parameter, from the corresponding Landau free energy (see *e.g.* Cao & Barsch, 1990; Houchmandzadeh *et al.*, 1991; Ishibashi, 1992, 1993; Rychetský & Schranz, 1993, 1994; Schranz, 1995; Huang *et al.*, 1997; Strukov & Levanyuk, 1998; Hatt & Hatch, 1999; Hatch & Cao, 1999).

Let us denote by $\mathsf{T}_{12}(\eta_1)$ the symmetry of the profile $\eta_1(\xi)$ and by $\mathsf{T}_{12}(\eta_2)$ the symmetry of the profile $\eta_2(\xi)$. Then the symmetry of the entire wall $\mathsf{T}_{12}(\eta)$ is a common part of the symmetries $\mathsf{T}_{12}(\eta_1)$ and $\mathsf{T}_{12}(\eta_2)$,

$$\mathsf{T}_{12}(\eta) = \mathsf{T}_{12}(\eta_1) \cap \mathsf{T}_{12}(\eta_2). \qquad (3.4.4.34)$$

Example 3.4.4.4. In our illustrative phase transition $4_z/m_z m_x m_{xy} \supset 2_x m_y m_z$, the order parameter has two components η_1, η_2 that can be associated with the x and y components P_1 and P_2 of the

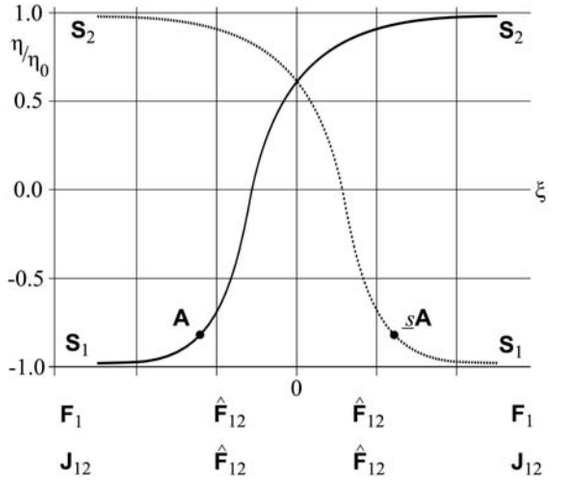

Fig. 3.4.4.9. Profiles of the one-component order parameter $\eta(\xi)$ in an asymmetric wall (solid curve) and in the reversed asymmetric wall (dotted curve). The wall is asymmetric and side-reversible (A$\underline{\rm R}$).

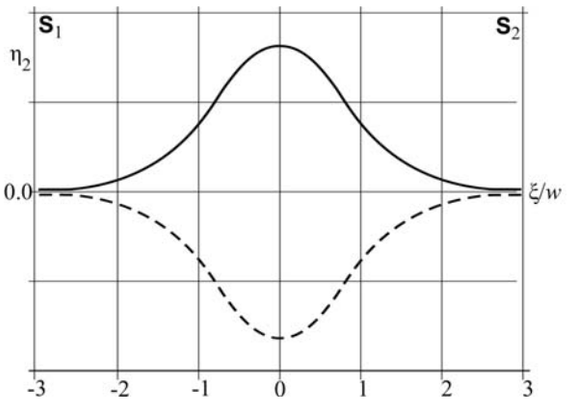

Fig. 3.4.4.10. A profile of the second order parameter component in a degenerate domain wall.

spontaneous polarization (see Table 3.1.3.1 and Fig. 3.4.2.2). We have seen that the domain wall $[\mathbf{S}_1[010]\mathbf{S}_2]$ of zero thickness has the symmetry $\mathsf{T}_{12} = \underline{2}_z^\star/m_z$. If one lets $\eta_1(y)$ relax and keeps $\eta_2(y) = 0$ (a so-called *linear structure*), then $\mathsf{T}_{12}(\eta_1) = \underline{2}_z^\star/m_z$ (see Fig. 3.4.4.2 with $\xi = y$). If the last condition is lifted, a possible profile of a relaxed $\eta_2(y)$ is depicted by the full curve in Fig. 3.4.4.10. If both components $\eta_1(y)$ and $\eta_2(y)$ are nonzero within the wall, one speaks about a *rotational structure* of domain wall. In this relaxed domain wall the spontaneous polarization rotates in the plane (001), resembling thus a Néel wall in magnetic materials. The even profile $\eta_2(-y) = \eta_2(y)$ has the symmetry $\mathsf{T}_{12}(\eta_2) = m_x^\star 2_y^\star m_z$. Hence, according to (3.4.4.34), the symmetry of a relaxed wall with a rotational structure is $\mathsf{T}_{12}(\eta) = \underline{2}_z^\star/m_z \cap m_x^\star 2_y^\star m_z = \{1, m_z\}$. This is an asymmetric state-reversible (AR*) wall with two chiral variants [see equation (3.4.4.33)] that are related by $\underline{1}^\star$ and $\underline{2}_z^\star$; the profile $\eta_2(y)$ of the second variant is depicted in Fig. 3.4.4.10 by a dashed curve.

Similarly, one gets for a zero-thickness domain wall $[\mathbf{S}_1[001]\mathbf{S}_2]$ perpendicular to z the symmetry $\mathsf{T}_{12} = \underline{2}_y^\star/m_y$. For a relaxed domain wall with profiles $\eta_1(z)$ and $\eta_2(z)$, displayed in Figs. 3.4.4.6 and 3.4.4.10 with $\xi = z$, one gets $\mathsf{T}_{12}(\eta_1) = \underline{2}_y^\star/m_y$, $\mathsf{T}_{12}(\eta_2) = m_x^\star 2_y^\star m_z$ and $\mathsf{T}_{12}(\eta) = \{1, \underline{2}_y^\star\}$. The relaxed domain wall with rotational structure has lower symmetry than the zero-thickness wall or the wall with linear structure, but remains a symmetric and reversible (SR) domain wall in which spontaneous polarization rotates in a plane (001), resembling thus a Bloch wall in magnetic materials. Two chiral right-handed and left-handed variants are related by operations m_z and $\underline{1}^\star$. This example illustrates that the structure of domain walls may differ with the wall orientation.

We note that the stability of a domain wall with a rotational structure and with a linear structure depends on the values of the coefficients in the Landau free energy, on temperature and on external fields. In favourable cases, a phase transition from a symmetric linear structure to a less symmetric rotational structure can occur. Such phase transitions in domain walls have been studied theoretically by Bul'bich & Gufan (1989*a*,*b*) and by Sonin & Tagancev (1989).

3.4.4.7. *Microscopic structure and symmetry of domain walls*

The thermodynamic theory of domain walls outlined above is efficient in providing quantitative results (wall thickness, energy) in any specific material. However, since this is a continuum theory, it is not able to treat local structural changes on a microscopic level and, moreover, owing to the small thickness of domain walls (several lattice constants), the reliability of its conclusions is to some extent uncertain.

Discrete theories either use simplified models [*e.g.* pseudospin ANNNI (axial next nearest neighbour Ising) model] that yield quantitative results on profiles, energies and interaction energies of walls but do not consider real crystal structures, or calculate numerically for a certain structure the atomic positions within a wall from interatomic potentials.

Symmetry analysis of domain walls provides useful qualitative conclusions about the microscopic structure of walls. Layer groups with discrete two-dimensional translations impose, *via* the site symmetries, restrictions on possible displacements and/or ordering of atoms or molecules. From these conclusions, combined with a reasonable assumption that these shifts or ordering vary continuously within a wall, one gets *topological constraints on the field of local displacements and/or ordering of atoms or molecules in the wall*. The advantage of this treatment is its simplicity and general validity, since no approximations or simplified models are needed. The analysis can also be applied to domain walls of zero thickness, where thermodynamic theory fails. However, this method does not yield any quantitative results, such as values of displacements, wall thickness, energy *etc.*

The procedure is similar to that in the continuum description. The main relations equations (3.4.4.12)–(3.4.4.17) and the classification given in Table 3.4.4.3 hold for a microscopic description as well; one has only to replace point groups by space groups.

A significant difference is that the sectional layer groups and the wall symmetry depend on the location of the plane p in the crystal lattice. This position can by expressed by a vector $s\mathbf{d}$, where $\mathbf{d}$ is the *scanning vector* (see *IT* E, 2002 and the example below) and s is a non-negative number smaller than 1, $0 \leq s < 1$. An extended symbol of a twin in the microscopic description, corresponding to the symbol (3.4.4.1) in the continuum description, is

$$(\mathsf{S}_1|\mathbf{n}; s\mathbf{d}|\mathsf{S}_2) \equiv (\mathsf{S}_2|-\mathbf{n}; s\mathbf{d}|\mathsf{S}_1). \qquad (3.4.4.35)$$

The main features of the analysis are demonstrated on the following example.

Example 3.4.4.5. Ferroelastic domain wall in calomel. We examine a ferroelastic compatible domain wall in a calomel crystal (Janovec & Zikmund, 1993; *IT* E, 2002, Chapter 5). In Section 3.4.2.5, Example 3.4.2.7, we found the microscopic domain states (see Fig. 3.4.2.5) and, in Section 3.4.3.7, the corresponding ordered domain pair $(\mathsf{S}_1, \mathsf{S}_3)$ and unordered domain pair $\{\mathsf{S}_1, \mathsf{S}_3\}$ (depicted in Fig. 3.4.3.10). These pairs have symmetry groups $\mathcal{F}_{13} = Pn_{x\bar{y}}n_{xy}m_z$ and $\mathcal{J}_{13} = P4_{2z}^\star/m_z n_{xy} m_x^\star$, respectively. Both groups have an orthorhombic basis $\mathbf{a}^o = \mathbf{a}^t - \mathbf{b}^t$, $\mathbf{b}^o = \mathbf{a}^t + \mathbf{b}^t$, $\mathbf{c}^o = \mathbf{c}^t$, with a shift of origin $\mathbf{b}^t/2$ for both groups.

Compatible domain walls in this ferroelastic domain pair have orientations (100) and (010) in the tetragonal coordinate system (see Table 3.4.3.6). We shall examine the former case – the latter is crystallographically equivalent. Sectional layer groups of this plane in groups $\mathcal{F}_{13}$ and $\mathcal{J}_{13}$ have a two-dimensional translation group (net) with basic vectors $\mathbf{a}^s = 2\mathbf{b}^t$ and $\mathbf{b}^s = \mathbf{c}^t$, and the scanning vector $\mathbf{d} = 2\mathbf{a}^t$ expresses the repetition period of the layer structure (*cf.* Fig. 3.4.3.10*a*). From the diagram of symmetry elements of the group $\mathcal{F}_{13}$ and $\mathcal{J}_{13}$, available in *IT* A (2002), one can deduce the sectional layer groups at any location $s\mathbf{d}$, $0 \leq s < 1$. These sectional layer groups are listed explicitly in *IT* E (2002) in the *scanning tables* of the respective space groups.

The resulting sectional layer groups $\overline{\mathcal{F}}_{13}$ and $\overline{\mathcal{J}}_{13}$ are given in Table 3.4.4.7 in two notations, in which the letter p signifies a two-dimensional net with the basic translations $\mathbf{a}^s$, $\mathbf{b}^s$ introduced above. Standard symbols are related to the basis $\mathbf{a}^s$, $\mathbf{b}^s$, $\mathbf{c}^s = \mathbf{d}$. Subscripts in non-coordinate notation specify the orientation of symmetry elements in the reference Cartesian coordinate system of the tetragonal phase, the partial translation in the glide plane a and in the screw axis 2_1 is equal to $\frac{1}{2}\mathbf{a}^s = \mathbf{b}^t$, *i.e.* the symbols a and 2_1 are also related to the basis $\mathbf{a}^s$, $\mathbf{b}^s$, $\mathbf{c}^s$. At special locations $s\mathbf{d} = 0\mathbf{d}$, $\frac{1}{2}\mathbf{d}$ and $s\mathbf{d} = \frac{1}{4}\mathbf{d}$, $\frac{3}{4}\mathbf{d}$, sectional groups contain both side-

Table 3.4.4.7. *Sectional layer groups and twin (wall) symmetries of the twin* $(\mathsf{S}_1|[100]; s\mathbf{d}|\mathsf{S}_3)$ *in a calomel crystal*

Location $s\mathbf{d}$	$\overline{\mathcal{F}}_{13}$		$\overline{\mathcal{J}}_{13}$		T_{13}		
	Standard	Non-coordinate	Standard	Non-coordinate	Standard	Non-coordinate	Classification
$\frac{1}{4}\mathbf{d}, \frac{3}{4}\mathbf{d}$	$p12/m1$	$p2_z/m_z$	$pmma$	$pm^\star_y m_z a^\star_x$	$p2_1ma$	$p2^\star_{1y} m_z a^\star_x$	SR
$0\mathbf{d}, \frac{1}{4}\mathbf{d}$	$p12/m1$†	$p2_z/m_z$†	$pmmm$†	$pm^\star_y m_z m^\star_x$†	$p2mm$	$p2^\star_y m_z m^\star_x$	SR
$s\mathbf{d}$	$p1m1$	pm_z	$pmm2$	$p2^\star_x m^\star_y m_z$	$p1m1$	pm_z	AR*

† Shift of origin $\mathbf{b}_t/2$.

preserving and side-reversing operations, whereas for any other location $s\mathbf{d}$ these layer groups are trivial (face) layer groups consisting of side-preserving operations only and are, therefore, also called *floating groups* in the direction $\mathbf{d}$ (*IT* E, 2002).

The wall (twin) symmetry T_{13} can be easily deduced from sectional layer groups $\overline{\mathcal{F}}_{13}$ and $\overline{\mathcal{J}}_{13}$: the floating group $\widehat{\mathcal{F}}_{13}$ is just the sectional layer group $\overline{\mathcal{F}}_{13}$ at a general location, $\widehat{\mathcal{F}}_{13} = \overline{\mathcal{F}}_{13}(s\mathbf{d}) = pm_z$. Two other generators in the group symbol of T_{13} are non-trivial twinning operations (underlined with a star) of $\overline{\mathcal{J}}_{13}$. The classification in the last column of Table 3.4.4.7 is defined in Table 3.4.4.3.

Local symmetry exerts constraints on possible displacements of the atoms within a wall. The site symmetry of atoms in a wall of zero thickness, or at the central plane of a finite-thickness domain wall, are defined by the layer group T_{13}. The site symmetry of the off-centre atoms at $0 < |\xi| < \infty$ are determined by floating group $\widehat{\mathcal{F}}_{13}$ and the limiting structures at $\xi \to -\infty$ and $\xi \to \infty$ by space groups $\mathcal{F}_1$ and $\mathcal{F}_3$, respectively. A reasonable condition that the displacements of atoms change continuously if one passes through the wall from $\xi \to -\infty$ to $\xi \to \infty$ allows one to deduce a qualitative picture of the displacements within a wall.

Symmetry groups of domain pairs, sectional layer groups and the twin symmetry have been derived in the parent clamping approximation (PCA) (see Section 3.4.2.5). As can be seen from Fig. 3.4.3.5, a relaxation process, accompanying a lifting of this approximation, consists of a simple shear (shear vector parallel to $\mathbf{q}$) and an elongation (or contraction) in the domain wall along the shear direction (change of the vector $\overrightarrow{AB}_0$ into the vector AB_1^+). These deformations influence neither the layer group T_{13} nor its floating group $\widehat{\mathcal{F}}_{13}$. Hence *the wall (twin) symmetry* T_{13} *derived in the parent clamping approximation expresses also the symmetry of a ferroelastic domain wall (twin) with nonzero spontaneous shear unless the simple shear is accompanied by a reshuffling of atoms or molecules in both domains*. This useful statement holds for any ferroelastic domain wall (twin).

A microscopic structure of the ferroelastic domain wall in two symmetrically prominent positions is depicted in Fig. 3.4.4.11. For better recognition, displacements of molecules are exaggerated and the changes of the displacement lengths are neglected. Since the symmetry of all groups involved contains a reflection m_z, the atomic shifts are confined to planes (001). It can be seen in the figure that when one moves through the wall in the direction [110] or [1$\bar{1}$0], the vector of the molecular shift experiences rotations through $\frac{1}{2}\pi$ about the $\mathbf{c}^t$ direction in opposite senses for the 'black' and 'white' molecules.

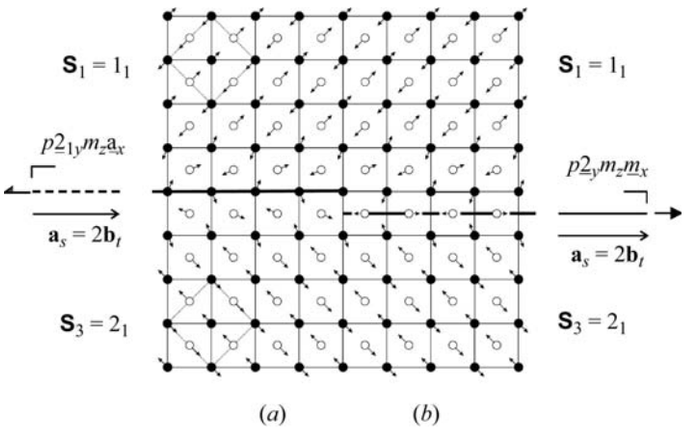

Fig. 3.4.4.11. Microscopic structure of a ferroelastic domain wall in calomel. (*a*) and (*b*) show a domain wall at two different locations with two different layer groups and two different structures of the central planes.

The 'black' molecules in the central layer at location $\frac{1}{4}\mathbf{d}$ or $\frac{3}{4}\mathbf{d}$ [wall (*a*) on the left-hand side of Fig. 3.4.4.11] exhibit nearly antiparallel displacements perpendicular to the wall. Strictly perpendicular shifts would represent 'averaged' displacements compatible with the layer symmetry $\overline{\mathcal{J}}_{13} = p2^\star_{1y} m_z a^\star_x$, which is, however, broken by a simple shear that decreases the symmetry to $\mathsf{T}_{13} = p2^\star_{1y} m_z a^\star_x$, which does not require perpendicular displacements of 'black' molecules.

The wall with central plane location $0\mathbf{d}$ or $\frac{1}{4}\mathbf{d}$ (Fig. 3.4.4.11*b*) has symmetry $\mathsf{T}_{13} = p2^\star_y m_z m^\star_x$, which restricts displacements of 'white' molecules of the central layer to the y direction only; the 'averaged' displacements compatible with $\overline{\mathcal{J}}_{13} = pm^\star_y m_z m^\star_x$ (origin shift $\mathbf{b}^t/2$) would have equal lengths of shifts in the $+y$ and $-y$ directions, but the relaxed central layer with symmetry $\mathsf{T}_{13} = p2^\star_y m_z m^\star_x$ allows unequal shifts in the $-y$ and $+y$ directions.

Walls (*a*) and (*b*) with two different prominent locations have different layer symmetries and different structures of the central layer. These two walls have extremal energy, but symmetry cannot decide which one has the minimum energy. The two walls have the same polar point-group symmetry $m^\star_x 2^\star_y m_z$, which permits a spontaneous polarization along y.

Similar analysis of the displacement and ordering fields in domain walls has been performed for KSCN crystals (Janovec *et al.*, 1989), sodium superoxide NaO_2 (Zieliński, 1990) and for the simple cubic phase of fullerene C_{60} (Saint-Grégoire *et al.*, 1997).

3.4.5. Glossary

Note: the correspondence between contracted Greek indices and the Cartesian vector components used in Sections 3.1.3, in the present chapter and in the software *GI⋆KoBo*-1, is defined in the following way:

Cartesian components	11	22	33	23, 32	31, 13	12, 21
Contracted notation	1	2	3	4	5	6

In this designation, coefficients with contracted indices 4, 5, 6 appear two times, *e.g.* index 4 replaces yz in one coefficient and zy in the other coefficient. With this convention, the coefficients transform in tensor space as vector components, but some coefficients differ from the usual matrix notation (Voigt matrices) by numerical factors [see Section 1.1.4.10; Nye (1985); Sirotin & Shaskolskaya, Appendix E (1982)].

(*a*) Objects

B_m	domain region
$\mathbf{d}$	scanning vector (basis vector of a scanning group)
$\mathbf{D}_i(\mathbf{S}_k, B_m)$	the ith domain, with domain state $\mathbf{S}_k$ in the mth domain region $\mathcal{B}_m$
$G\mathbf{S}_1$	G-orbit of principal single-domain states